Symmetric Box-Splines on Root Lattices

Minho Kim

School of Computer Science, University of Seoul, Siripdae-gil 13, Dongdaemun-gu, Seoul, 130-743, Republic of Korea

Jörg Peters

Department of CISE, University of Florida, CSE Bldg., University of Florida, Gainesville, FL, 32611, USA

Abstract

Root lattices are efficient sampling lattices for reconstructing isotropic signals in arbitrary dimensions, due to their highly symmetric structure. One root lattice, the Cartesian grid, is almost exclusively used since it matches the coordinate grid; but it is less efficient than other root lattices. *Box-splines*, on the other hand, generalize tensor-product B-splines by allowing non-Cartesian directions. They provide, in any number of dimensions, higher-order reconstructions of fields, often of higher efficiency than tensored B-splines. But on non-Cartesian lattices, such as the BCC (Body-Centered Cubic) or the FCC (Face-Centered Cubic) lattice, only some box-splines and then only up to dimension three have been investigated.

This paper derives and completely characterizes efficient symmetric box-spline reconstruction filters on *all irreducible root lattices* that exist *in any number of dimensions* $n \geq 2$ ($n \geq 3$ for $\mathcal{D}_n$ and $\mathcal{D}_n^*$ lattices). In all cases, box-splines are constructed by convolution using the lattice directions, generalizing the known constructions in two and three variables. For each box-spline, we document the basic properties for computational use: the polynomial degree, the continuity, the linear independence of shifts on the lattice and optimal quasi-interpolants for fast approximation of fields.

Keywords: Box-spline, Root lattice, Sampling lattice, Reconstruction filter, Multi-dimensional signal processing, Approximation, Quasi-interpolation

1. Introduction

Given discrete samples on a sampling lattice, the task of signal processing is to reconstruct the original signal by recovering its primal spectrum with a proper *reconstruction filter*, i.e. to approximate regularly spaced data from a corresponding space of functions. In one variable there is only one type of *uniform sampling lattice* and the filter alone determines the quality of the reconstruction. But in higher dimensions, the choice of sampling lattice plays as important a role as the choice of filter. While the best sampling lattice depends on the individual input signal, it is not practical to use a different sampling lattice for each input signal and we usually cannot predict the signal. Therefore sampling lattices are chosen based on standard

Email addresses: `minhokim@uos.ac.kr` (Minho Kim), `jorg@cise.ufl.edu` (Jörg Peters)

assumptions: that the input signal is *band-limited* and its spectrum is *isotropic*. Under these assumptions, the *optimal sampling lattice* is the one of lowest density so that the signal can be reconstructed without aliasing by a canonical filter. This lattice is the dual of the solution to the densest sphere packing problem on lattices [1]. *Root lattices*, i.e. lattices invariant under Euclidean reflection groups, are prominent among the known densest sphere packing lattices. The self-dual Cartesian grid is a root lattice but has comparatively low sampling efficiency since, as Figure 1 indicates, it has the least density of the root lattices.

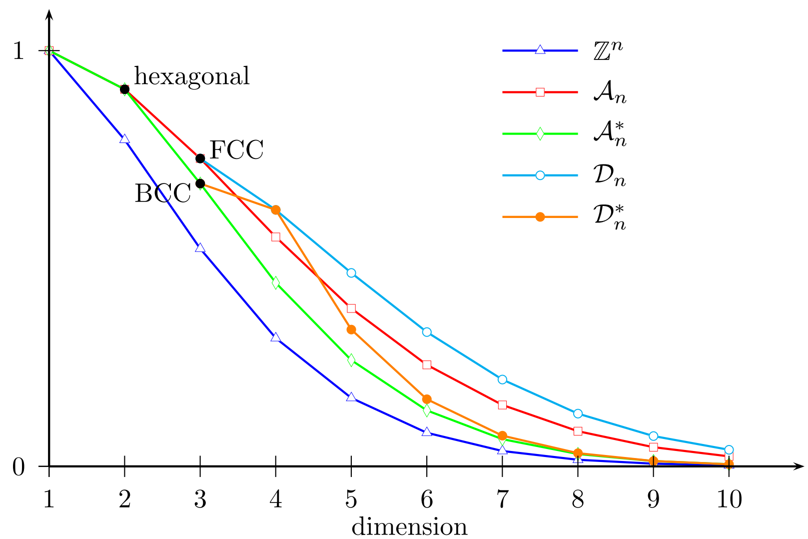

Figure 1. Density of root lattices up to dimension 10. The relative density of $\mathbb{Z}^n$ compared to $\mathcal{D}_n$ for $n = 3, 4, 5, 6$ decreases as 71%, 50%, 35%, 25%, respectively.

For example, the BCC root lattice can reduce the number of samples by 29% compared to a Cartesian lattice without any loss of information [2]. Figure 1 shows that the savings increase in more than three dimensions.

In dimensions two and three, specific root lattices have been exploited by efficient symmetric reconstruction filters: splines on the hexagonal lattice [3], the 7-direction trivariate box-spline on the Cartesian lattice [4, 5], box-splines on the BCC lattice [6], and 6-direction trivariate box-spline on the FCC lattice [7, 8] (see [9] for a broad literature review). But for higher dimensions, only the n-dimensional Cartesian lattice readily offers efficient symmetric reconstruction filters in the form of tensor-product B-splines.

In this paper, we show that *multivariate box-splines*, a generalization of (univariate) uniform B-splines to multiple variables, provide a natural match on other root lattices. As piecewise polynomials defined by consecutive integer-directional convolutions, these box-splines can possess higher continuity and higher approximation order for a given *total polynomial degree*, than tensor-product B-splines (see Table 1).

Overview. In this paper we derive families of symmetric box-splines in *any number of dimensions* for *all irreducible root lattices*. Such constructions are facilitated by defining simple square generator matrices. Specifically, we first derive a non-tensored family of filters on the Cartesian lattice (Section 3) and then

lattice	approx. order	total degree	
		box-spline	B-spline
$\mathbb{Z}^n$	$2^{n-2}+2$	2^{n-1}	$n(2^{n-2}+1)$
$\mathcal{A}_n$	n	$\frac{n(n-1)}{2}$	$n(n-1)$
$\mathcal{A}_n^*$	$2r$	$r(n+1)-n$	$n(2r-1)$
$\mathcal{D}_n$	$2n-2$	$n(n-2)$	$n(2n-3)$
$\mathcal{D}_n^*$	$2^{n-2}+2$	2^{n-1}	$n(2^{n-2}+1)$

Table 1. Approximation order and polynomial degree for symmetric box-splines on root lattices compared to tensor-product B-splines for dimension $n \geq 2$ for $\mathbb{Z}^n$, $\mathcal{A}_n$ and $\mathcal{A}_n^*$ and $n \geq 3$ for $\mathcal{D}_n$ and $\mathcal{D}_n^*$.

address the $\mathcal{A}_n$ lattice, its dual $\mathcal{A}_n^*$ and the $\mathcal{D}_n$ lattice and its dual $\mathcal{D}_n^*$ (see Table 2). We only leave out the irreducible root lattices $\mathcal{E}_6$, $\mathcal{E}_7$, $\mathcal{E}_8$ and their duals since they are specific to dimensions 6,7 and 8, respectively. For each box-spline, we document its polynomial degree, continuity, optimal approximation order and the linear independence of shifts on the lattice; and we exhibit optimal quasi-interpolants, i.e. simple rules for determining box-spline coefficients from data, that allow efficient construction of fields that approximate the original field up to a given order (Section 2.3). Table 2 gives an overview of the lattices and Table 3 provides a succinct summary of all results for lattice-and-box-spline-family pairs.

2. Background: Notation, Root Lattices and Box-Splines

2.1. Notation

Matrices, including the box-spline direction matrices (e.g., $\mathbf{\Xi}$ and $\mathbf{T}_r$) and the lattice generator matrices (e.g., $\mathbf{G}$, $\mathbf{A}_{\mathrm{P}}^*$ and $\mathbf{A}_n^{\pm}$), are typeset in bold upper case; vectors are typeset in bold lower case, in (i) italic if variable, e.g., $\boldsymbol{x}$ and $\boldsymbol{j}$, and (ii) non-italic if constant, e.g., $\mathbf{e}_n^j$ and $\mathbf{j}_n$; lattices are typeset in calligraphic upper case; e.g., $\mathcal{A}_n$ and $\mathcal{D}_n$ and root systems and finite reflection (Coxeter) groups are typeset as, e.g., $\mathscr{A}_n$ and $\mathscr{D}_n$. The dimension of vectors and matrices is indicated by a subscript when not obvious from the context. We note in particular, $\boldsymbol{x}(j)$, $1 \leq j \leq n$, is the j-th element of the vector $\boldsymbol{x} \in \mathbb{R}^n$, $\mathbf{e}_n^j$ the j-th unit vector in $\mathbb{R}^n$, $\mathbf{I}_n$ the $n \times n$ identity matrix, $\mathbf{0}_n := [0 \cdots 0]^t$ the n-dimensional zero vector, $\mathbf{j}_n := [1 \cdots 1]^t$ the 'diagonal vector', $\mathbf{J}_n := \mathbf{j}_n\mathbf{j}_n^t$ the $n \times n$ matrix composed of 1's only and $\mathbf{P}_n := \mathbf{I}_n - \mathbf{J}_n/n : \mathbb{R}^n \to H_{\mathbf{j}}^{n-1}$ is the orthogonal projection along $\mathbf{j}_n$ onto the plane $H_{\mathbf{j}}^{n-1}$ where, with the dot product $\boldsymbol{x} \cdot \boldsymbol{y} := \boldsymbol{x}^t\boldsymbol{y} \in \mathbb{R}$, $H_{\mathbf{j}}^{n-1} := \{\boldsymbol{x} \in \mathbb{R}^n : \boldsymbol{x} \cdot \mathbf{j}_n = 0\}$ is the $(n-1)$-dimensional hyperplane embedded in $\mathbb{R}^n$ intersecting $\mathbf{0}$ with normal $\mathbf{j}_n$. Following the convention in [11], an $n \times m$ matrix will be interpreted as a collection of column vectors or as a linear transformation from $\mathbb{R}^m$ to $\mathbb{R}^n$. When interpreted as a set of column vectors, repeated columns are considered different elements. Column vectors are used as either vectors or points depending on

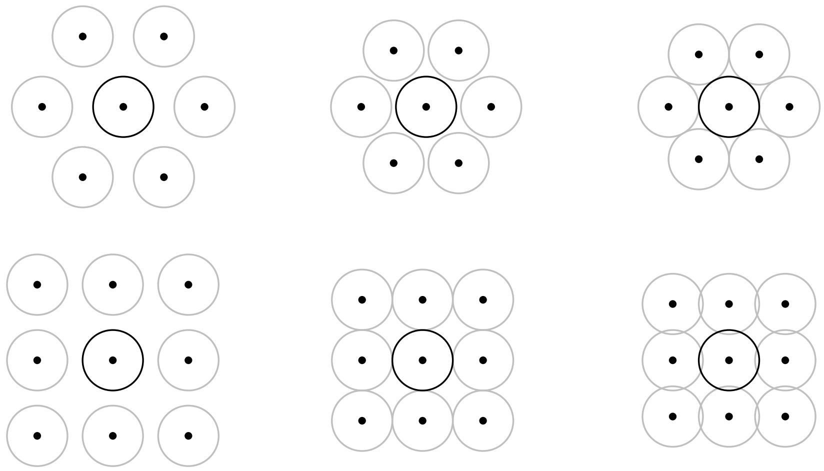

Figure 2. Unit 'ball' (primary spectrum and its replicas) packing with respect to the density δ for (top) the hexagonal lattice and (bottom) the Cartesian lattice. (left) Sampling density is high enough so that no pair of spectra overlap; (bottom center) the primary spectrum and its replicas touch on the Cartesian lattice but (top center) are separated on the hexagonal lattice; (top right) the balls only touch on the hexagonal lattice, and hence the original signal still can be reconstructed without aliasing. (bottom right) On the Cartesian lattice the spectra overlap, causing aliasing.

the context. $\#A$ denotes the cardinality of the set A. A matrix $\mathbf{U} \in \mathbb{Z}^{n\times m}$ is *unimodular* if $\det \mathbf{Z} \in \{-1, 1, 0\}$ for all square submatrices $\mathbf{Z} \subseteq \mathbf{U}$. If $\mathbf{U} \in \mathbb{Z}^{n\times n}$ is unimodular and invertible then $\mathbf{U}^{-1} \in \mathbb{Z}^{n\times n}$.

2.2. Lattices and sampling

An n-dimensional *lattice* $\mathcal{L}_n$ embedded in $\mathbb{R}^l, l \geq n$ is a discrete subgroup generated by a $l \times n$ *generator matrix* $\mathbf{G}$ of $\operatorname{rank}(\mathbf{G}) = n$ [12]:

$$\mathcal{L}_n := \{\mathbf{G}\boldsymbol{j} \in \mathbb{R}^l : \boldsymbol{j} \in \mathbb{Z}^n\}.$$

That is, all integer linear combinations $\mathbf{G}\mathbb{Z}^n$ define (the points of) the n-dimensional lattice. Any n-dimensional lattice $\mathcal{L}_n$ has a *dual* lattice given by

$$\mathcal{L}_n^* := \left\{\boldsymbol{x} \in \mathbb{R}^l : \boldsymbol{x} \cdot \boldsymbol{u} \in \mathbb{Z}, \forall \boldsymbol{u} \in \mathcal{L}_n\right\}.$$

Lattices obtained from one another by a rotation, reflection and change of uniform scale are said to be *equivalent*, written $\cong$ [10]. Table 2 summarizes the root lattices relevant for this paper.

The *density* of a lattice packing is the proportion of the space occupied by the spheres when packed. The *center density* of a lattice is the number of the lattice points per unit volume, which can be obtained by dividing its density by the volume of the unit sphere [10]. Figure 2 illustrates how the sampling efficiency differs according to packing density of the lattice: If the density of the dual lattice is sufficiently low, and

Table 2. Domain lattices (see Section 2.1 for the notation) [10]

lattice	generator matrix	center density	root system	symmetry order	Coxeter diagram
$\mathbb{Z}^n$	$\mathbf{I}_n$	2^{-n}	$\mathscr{B}_n$	$2^n n!$	
$\mathcal{A}_n$	$\mathbf{A}_n^{\pm} := \mathbf{I}_n + \left(-1 \pm \sqrt{n+1}\right) \frac{\mathbf{J}_n}{n}$	$2^{-n/2}(n+1)^{-1/2}$	$\mathscr{A}_n$	$(n+1)!2$	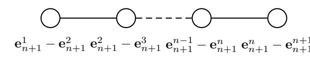
$\mathcal{A}_n^*$	$\mathbf{A}_n^{*\pm} := \mathbf{I}_n + \left(-1 \pm \frac{1}{\sqrt{n+1}}\right) \frac{\mathbf{J}_n}{n}$	$\dfrac{n^{n/2}}{2^n(n+1)^{(n-1)/2}}$			
$\mathcal{D}_n$	$\mathbf{G}_{\mathcal{D}_n} := \begin{bmatrix} \mathbf{I}_{n-1} & -\mathbf{e}_n^{n-1} \\ -\mathbf{j}_{n-1}^t & -1 \end{bmatrix}$	$2^{-(n+2)/2}$	$\mathscr{C}_n$ or $\mathscr{D}_n$	$\begin{cases} 2^n n! & (n \neq 4) \\ 1152 & (n = 4) \end{cases}$	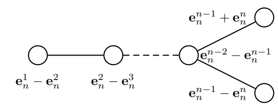
$\mathcal{D}_n^*$	$\mathbf{G}_{\mathcal{D}_n^*} := \begin{bmatrix} \mathbf{I}_{n-1} & \mathbf{j}_{n-1}/2 \\ \mathbf{0}_{n-1}^t & 1/2 \end{bmatrix}$	$\begin{cases} 3^{1.5}2^{-5} & (n=3) \\ 2^{-(n-1)} & (n>3) \end{cases}$			

accordingly the sampling density high as in the leftmost case, then the original signal can be reconstructed without aliasing regardless of the sampling lattice; but, as can be seen from the rightmost case, when sampled sparsely, aliasing, visible as overlap of the primary disk-shaped spectrum and its replicas, depends on the sampling lattice. Therefore, larger (center) density implies that *its dual is a more efficient sampling lattice.* Table 2 (middle column) shows the center density of the root lattices considered in our paper. When plotted (see Figure 1), this reveals the Cartesian lattice $\mathbb{Z}^n$ to have the poorest sampling efficiency among the irreducible root lattices.

2.3. Box-Splines

We use the notation and definitions made standard by de Boor et al. [11]. (See also [13].) In particular, a box-spline is a smooth piecewise polynomial of finite support and a *spline* in box-spline form is a linear combination of the shifts of a box-spline. If the sequence of the shifts of a box-spline are linearly independent, the box-spline is a *basis* function.

Definition. Geometrically, the value of a box-spline with direction matrix $\boldsymbol{\Xi} \in \mathbb{R}^{n \times m}$ at $\boldsymbol{x} \in \operatorname{ran}\boldsymbol{\Xi} \subset \mathbb{R}^n$ is the shadow-density [11, (I.3)] (see, e.g., Figure 3 or Figure 6)

$$M_{\boldsymbol{\Xi}}(\boldsymbol{x}) := \operatorname{vol}_{m-\operatorname{rank}(\boldsymbol{\Xi})}\left(\boldsymbol{\Xi}^{-1}\{\boldsymbol{x}\} \cap \square\right) / |\det \boldsymbol{\Xi}|,$$

i.e., the normalized volume of the intersection of a half-open cube $\square := [0..1)^m \subset \mathbb{R}^m$, $m \geq n$, with the pre-image $\boldsymbol{\Xi}^{-1}\{\boldsymbol{x}\} := \{\boldsymbol{y} \in \mathbb{R}^m : \boldsymbol{\Xi}\boldsymbol{y} = \boldsymbol{x}\}$ of $\boldsymbol{x}$ under the $n \times m$ direction matrix $\boldsymbol{\Xi}$ possibly with repeated columns. This is an $(m - \dim \operatorname{ran}\boldsymbol{\Xi})$-dimensional affine subspace in $\mathbb{R}^m$ and $\operatorname{vol}_d(\cdot)$ is the d-dimensional volume of its argument. Alternatively, we can construct $M_{\boldsymbol{\Xi}}$ via consecutive directional convolutions along

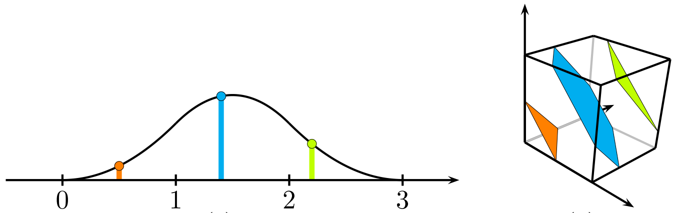

(a) (b)

Figure 3. Geometric definition of the box-spline with the direction matrix $\mathbf{\Xi} := [1\ 1\ 1]$; area of intersection of a cube with $\mathbf{\Xi}^{-1}\{x\} = [1\ 1\ 1]^t/3\{x\} + H^2_{\mathbf{j}}$, the translates of the hyperplanes orthogonal to $\mathbf{j}_3 := [1\ 1\ 1]^t$.

the directions in $\mathbf{\Xi}$ as in Figure 4 [11, (I.8)]:

$$M_{\mathbf{\Xi}\cup\boldsymbol{\zeta}} = \int_0^1 M_{\mathbf{\Xi}}(\cdot - t\boldsymbol{\zeta})dt.$$

In the following, unless mentioned specifically, we assume $\operatorname{rank}(\mathbf{\Xi}) = n$, hence the subspace spanned by the columns of $\mathbf{\Xi}$, $\operatorname{ran}\mathbf{\Xi} = \mathbb{R}^n$.

Polynomial Degree, Continuity and Cardinal Spline Space. A box-spline $M_{\mathbf{\Xi}}$ is a piecewise polynomial on $\operatorname{ran}\mathbf{\Xi}$. Its polynomial degree is less than or equal to $\#\mathbf{\Xi} - n$. The polynomial pieces join to form a function in $C^{m-1}(\operatorname{ran}\mathbf{\Xi})$ where [11, page 9]

$$m := m(\mathbf{\Xi}) := \min\{\#\mathbf{Z} : \mathbf{Z} \in \mathcal{A}(\mathbf{\Xi})\} - 1 \tag{1}$$

and [11, page 8] $\mathcal{A}(\mathbf{\Xi}) := \{\mathbf{Z} \subseteq \mathbf{\Xi} : \mathbf{\Xi}\backslash\mathbf{Z} \text{ does not span } \mathbb{R}^n\}$. The cardinal spline space [11, (II.1)]

$$S_{\mathbf{\Xi}} := \operatorname{span}\left(M_{\mathbf{\Xi}}(\cdot - \boldsymbol{j})\right)_{\boldsymbol{j}\in\mathbb{Z}^n}$$

is the spline space spanned by the shifts of $M_{\mathbf{\Xi}}$ on $\mathbb{Z}^n$. Each spline $s \in S_{\mathbf{\Xi}}$ has the form $s := \sum_{\boldsymbol{j}\in\mathbb{Z}^n} M_{\mathbf{\Xi}}(\cdot - \boldsymbol{j})a(\boldsymbol{j})$ with a mesh function (spline coefficients) $a : \mathbb{Z}^n \to \mathbb{R}$. The sequence $\left(M_{\mathbf{\Xi}}(\cdot - \boldsymbol{j})\right)_{\boldsymbol{j}\in\mathbb{Z}^n}$ is linearly independent if and only if $\mathbf{\Xi}$ is *unimodular* [11, page 41].

Quasi-Interpolation. A quasi-interpolant for the spline space $S_{\mathbf{\Xi}}$ provides a fast way of approximating a function f by a spline $Q_{M_{\mathbf{\Xi}}} f \in S_{\mathbf{\Xi}}$. We focus on quasi-interpolants that provide the optimal approximation order $m(\mathbf{\Xi}) + 1$ by *reproducing* polynomial terms up to degree $m(\mathbf{\Xi})$ [11, page 72]:

$$(Q_{M_{\mathbf{\Xi}}} f)(\boldsymbol{x}) := \sum_{\boldsymbol{j}\in\mathbb{Z}^n} M_{\mathbf{\Xi}}(\boldsymbol{x} - \boldsymbol{j})\lambda_{M_{\mathbf{\Xi}}}\left(f(\cdot + \boldsymbol{j})\right). \tag{2}$$

Here $\lambda_{M_{\mathbf{\Xi}}}$ is the linear functional [11, (III.22)]

$$\lambda_{M_{\mathbf{\Xi}}} f := \sum_{|\boldsymbol{\alpha}|\le m(\mathbf{\Xi})} g_{\boldsymbol{\alpha}}(\mathbf{0})\left(D^{\boldsymbol{\alpha}} f\right)(\mathbf{0}) \tag{3}$$

and $\boldsymbol{\alpha} \in \mathbb{Z}^n_+$ is a multi-index. The *Appell sequence* $\{g_{\boldsymbol{\alpha}}\}$ in (3) can be computed either recursively as

$$\begin{cases} g_{\mathbf{0}} = [\![]\!]^{\mathbf{0}} \\ g_{\boldsymbol{\alpha}} = [\![]\!]^{\boldsymbol{\alpha}} - \sum_{\boldsymbol{\beta}\neq\boldsymbol{\alpha}}(\mu_{\mathbf{\Xi}}[\![]\!]^{\boldsymbol{\alpha}-\boldsymbol{\beta}})g_{\boldsymbol{\beta}} \end{cases} \qquad \text{where } \mu_{\mathbf{\Xi}} f := \sum_{\boldsymbol{j}} M_{\mathbf{\Xi}}(\boldsymbol{j})f(-\boldsymbol{j}), \qquad ([11, (III.19)])$$

or from the Fourier transform $\widehat{M_{\boldsymbol{\Xi}}}$ as $g_{\boldsymbol{\alpha}}(\mathbf{0}) = \left([\![-iD]\!]^{\boldsymbol{\alpha}} \left(1/\widehat{M_{\boldsymbol{\Xi}}} \right) \right)(\mathbf{0})$. [11, (III.34)].

3. The Symmetric $(n+2^{n-1})$-direction Box-Spline on the Cartesian Lattice

Tensor-product B-splines are the most popular reconstruction filters on the Cartesian lattice. Their separable tensor structure simplifies computations, and shifts on the Cartesian lattice are linearly independent. But their continuity and approximation order are low for their total polynomial degree when compared to other box-splines. For example, the bi-quadratic B-spline and the ZP-element (Section 3.2) are both C^1 but their total degrees are 4 and 2, respectively.

We can construct other box-splines with higher approximation order for a given degree, by leveraging more directions of the Cartesian lattice. One way is to include the 2^{n-1} diagonal directions of the unit cube in addition to its n main axis directions. In dimension two, this results in the well-known Zwart-Powell element [14] (Table 3 and Figure 4) and in dimension three, it yields the 7-direction trivariate box-spline $M_{\mathbb{Z}^3}$ [4] (see Section 3.2).

3.1. Lattice, Definition and Properties

The root system $\mathscr{B}_n$ and the Cartesian lattice. The Cartesian lattice has been used as a sampling lattice for a long time, since it naturally matches the Cartesian coordinates. As one of the root lattices generated by the root system [15]

$$\mathscr{B}_n := \{\pm \mathbf{e}_n^i \pm \mathbf{e}_n^j : 1 \leq i \neq j \leq n\} \cup \bigcup_{1\leq j\leq n} \{\mathbf{e}_n^j\},$$

its symmetry group consists of all $n!$ permutations and 2^n sign changes of the coordinates. Hence the order is $2^n n!$ [10].

Box-spline $M_{\mathbb{Z}^n}$. Since the end points of the 2^n diagonals, $\{\boldsymbol{v} \in \mathbb{R}^n : \boldsymbol{v}(j) \in \{\pm 1\}, 1 \leq j \leq n\}$, map to one another under the operations of the symmetry group of $\mathscr{B}_n$, we can add these 2^{n-1} non-parallel diagonal directions and define the direction matrix

$$\boldsymbol{\Xi}_{\mathbb{Z}^n} := \mathbf{I}_n \cup \{\mathbf{e}_n^n + \sum_{j=1}^{n-1} \sigma_j \mathbf{e}_n^j : \sigma_j \in \{\pm 1\}\}, \quad n \geq 2.$$

This yields the centered box-spline

$$M_{\mathbb{Z}^n} := M^c_{\boldsymbol{\Xi}_{\mathbb{Z}^n}} = M_{\boldsymbol{\Xi}_{\mathbb{Z}^n}}(\cdot + \sum_{\boldsymbol{\xi}\in\boldsymbol{\Xi}_{\mathbb{Z}^n}} \boldsymbol{\xi}/2). \tag{4}$$

The following lemma will be helpful to prove the properties of $M_{\mathbb{Z}^n}$.

Lemma 1 (Independent directions)**.** *For a nonzero vector $\boldsymbol{v} \in \mathbb{R}^n$, let $\boldsymbol{\Xi}^{\perp \boldsymbol{v}} := \{\boldsymbol{\xi} \in \boldsymbol{\Xi} : \boldsymbol{\xi} \cdot \boldsymbol{v} = 0, \}$ be the vectors in $\boldsymbol{\Xi}$ orthogonal to $\boldsymbol{v}$. Then*

$$\max_{\boldsymbol{v}\in\mathbb{R}^n} \#\boldsymbol{\Xi}_{\mathbb{Z}^n}^{\perp \boldsymbol{v}} = 2^{n-2} + n - 2.$$

Proof. If we choose $\boldsymbol{v}^* := \mathbf{e}_n^n + \mathbf{e}_n^{n-1}$ then

$$\boldsymbol{\Xi}_{\mathbb{Z}^n}^{\perp \boldsymbol{v}^*} = \{\mathbf{e}_n^n - \mathbf{e}_n^{n-1} + \sum_{j=1}^{n-2} \pm \mathbf{e}_n^j\} \cup (\mathbf{I}_n \backslash \{\mathbf{e}_n^{n-1}, \mathbf{e}_n^n\})$$

and therefore $\#\boldsymbol{\Xi}_{\mathbb{Z}^n}^{\perp \boldsymbol{v}^*} = 2^{n-2} + n - 2$. To show that $2^{n-2} + n - 2$ is the upper bound, abbreviate $\mathbf{Z} := \{\mathbf{e}_n^n + \sum_{j=1}^{n-1} \sigma_j \mathbf{e}_n^j : \sigma_j \in \{\pm 1\}\}$ so that $\boldsymbol{\Xi}_{\mathbb{Z}^n} = \mathbf{Z} \sqcup \mathbf{I}_n$. Since the last entry of every column is 1, $\#\mathbf{Z} = 2^{n-1}$. Let $\mathbf{0} \neq \boldsymbol{v} \in \mathbb{R}^n$ be a vector with k nonzero entries. Since $\mathbf{Z}^{\perp \boldsymbol{v}} = \emptyset$ for $k = 1$, we consider only $k > 1$. We split

$$\mathbf{Z} = \mathbf{Z}_0 \sqcup \mathbf{Z}_1, \quad \text{where} \quad \mathbf{Z}_0 := \{\boldsymbol{\zeta} \in \mathbf{Z} : \boldsymbol{\zeta} \cdot \boldsymbol{v} = 0\} \quad \text{and} \quad \mathbf{Z}_1 := \{\boldsymbol{\zeta} \in \mathbf{Z} : \boldsymbol{\zeta} \cdot \boldsymbol{v} \neq 0\}.$$

Let $\boldsymbol{v}(i) \neq 0$, $i < n$ and $\boldsymbol{\zeta}_0$ and $\boldsymbol{\zeta}_1$ two columns that differ only in the (sign of the) i-th entry. Then $\boldsymbol{\zeta}_0 \in \mathbf{Z}_0$ implies $\boldsymbol{\zeta}_1 \in \mathbf{Z}_1$. Therefore $\mathbf{Z}_1$ has at least as many elements as $\mathbf{Z}_0$ and $\#\mathbf{Z}^{\perp \boldsymbol{v}} = \#\mathbf{Z}_0 \leq \#\mathbf{Z}/2 = 2^{n-2}$. Since $\#\mathbf{I}_n^{\perp \boldsymbol{v}} = n - k$, we get

$$\#\boldsymbol{\Xi}_{\mathbb{Z}^n}^{\perp \boldsymbol{v}} = \#\mathbf{Z}^{\perp \boldsymbol{v}} + \#\mathbf{I}_n^{\perp \boldsymbol{v}} \leq 2^{n-2} + n - k.$$

and the last expression is maximized when $k = 2$. □

Theorem 1 (Properties of $M_{\mathbb{Z}^n}$)**.** *The box-spline $M_{\mathbb{Z}^n}$ is (i) of total polynomial degree 2^{n-1}, (ii) $M_{\mathbb{Z}^n} \in C^{2^{n-2}}$ and (iii) the sequence $(M_{\mathbb{Z}^n}(\cdot - \boldsymbol{j}))_{\boldsymbol{j} \in \mathbb{Z}^n}$, $n \geq 2$, is linearly dependent.*

Proof. (i) The box-spline's degree follows from $\#\boldsymbol{\Xi}_{\mathbb{Z}^n} - n = n + 2^{n-1} - n = 2^{n-1}$.

(ii) By Lemma 1, at most $(2^{n-2} + n - 2)$ directions span a hyperplane. Therefore we have $m(\boldsymbol{\Xi}_{\mathbb{Z}^n}) = ((n + 2^{n-1}) - (2^{n-2} + n - 2)) - 1 = 2^{n-2} + 1$ and the claim follows by the remark preceding (1).

(iii) For the matrix

$$\mathbf{Z}_n := \bigcup_{i=1}^{n} \left\{ -\sum_{j=1}^{i-1} \mathbf{e}_n^j + \sum_{j=i}^{n} \mathbf{e}_n^j \right\} = \begin{bmatrix} 1 & -1 & \cdots & -1 & -1 \\ 1 & 1 & \cdots & -1 & -1 \\ \vdots & \vdots & \ddots & \vdots & \vdots \\ 1 & 1 & \cdots & 1 & -1 \\ 1 & 1 & \cdots & 1 & 1 \end{bmatrix} = \begin{bmatrix} 1 & 0 & \cdots & 0 & 0 \\ 1 & 1 & \cdots & 0 & 0 \\ \vdots & \vdots & \ddots & \vdots & \vdots \\ 1 & 1 & \cdots & 1 & 0 \\ 1 & 1 & \cdots & 1 & 1 \end{bmatrix} \begin{bmatrix} 1 & -1 & \cdots & -1 & -1 \\ 0 & 2 & \cdots & 0 & 0 \\ \vdots & \vdots & \ddots & \vdots & \vdots \\ 0 & 0 & \cdots & 2 & 0 \\ 0 & 0 & \cdots & 0 & 2 \end{bmatrix} \subset \boldsymbol{\Xi}_{\mathbb{Z}^n},$$

$\det \mathbf{Z}_n = 2^{n-1} \notin \{-1, 1, 0\}$ for $n \geq 2$, i.e. $\boldsymbol{\Xi}_{\mathbb{Z}^n}$ is not unimodular and the claim follows.

□

3.2. Examples

ZP-Element. In dimension two, $\boldsymbol{\Xi}_{\mathbb{Z}^2}$ is the direction matrix of the well-known ZP-element [14]:

$$\boldsymbol{\Xi}_{\mathrm{ZP}} := \begin{bmatrix} 1 & 0 & 1 & -1 \\ 0 & 1 & 1 & 1 \end{bmatrix} =: \boldsymbol{\Xi}_{\mathbb{Z}^2}.$$

Figure 4 shows the construction of the ZP-element via consecutive directional convolutions along the directions in $\boldsymbol{\Xi}_{\mathrm{ZP}}$. Note that the ZP-element is not centered whereas $M_{\mathbb{Z}^2}$ is centered by (4).

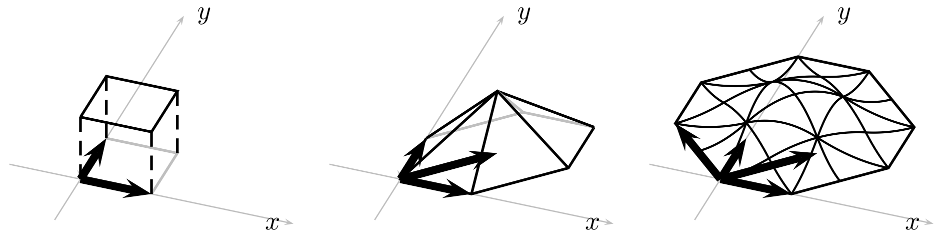

(a) $\left[\begin{smallmatrix}1&0\\0&1\end{smallmatrix}\right]$ (b) $\left[\begin{smallmatrix}1&0&1\\0&1&1\end{smallmatrix}\right]$ (c) $\left[\begin{smallmatrix}1&0&1&-1\\0&1&1&1\end{smallmatrix}\right]$

Figure 4. Construction of the ZP-element via directional convolutions.

The (total) degree of $M_{\mathbb{Z}^2}$ is $2^{2-1} = 2$ and $M_{\mathbb{Z}^2} \in C^{2^{2-2}} = C^1$. The BB(Bernstein-Bézier)-coefficients (the BB-net) [16] of $M_{\mathbb{Z}^2}$ can be found in [17]. Following the procedure laid out in [11, (III.22)], we derive the quasi-interpolant $Q_{\mathbb{Z}^2}$ with optimal approximation order 3 for the spline space $S_{\mathbb{Z}^2} := \operatorname{span}\left(M_{\mathbb{Z}^2}(\cdot - \boldsymbol{j})\right)_{\boldsymbol{j}\in\mathbb{Z}^2}$ as

$$\left(Q_{\mathbb{Z}^2} f\right)(\boldsymbol{x}) := \sum_{\boldsymbol{j}\in\mathbb{Z}^2} M_{\mathbb{Z}^2}(\boldsymbol{x}-\boldsymbol{j})\lambda_{\mathbb{Z}^2}\left(f(\cdot+\boldsymbol{j})\right). \tag{5}$$

An optimal choice of spline coefficients for data f is given by the functional

$$\begin{aligned}\lambda_{\mathbb{Z}^2} f := \lambda_{M_{\mathbb{Z}^2}} f &= (f - \frac{1}{8}(D_1^2 + D_2^2)f)(\mathbf{0}) = (f - \frac{1}{24}(D_1^2 + D_2^2 + (D_1 + D_2)^2 + (-D_1 + D_2)^2)f)(\mathbf{0}) \\ &= (f - \frac{1}{24}\sum_{\boldsymbol{\xi}\in\boldsymbol{\Xi}_{\mathrm{ZP}}} D_{\boldsymbol{\xi}}^2 f)(\mathbf{0}).\end{aligned}$$

Note that this functional differs from the one in [11, III(23)] since $M_{\mathbb{Z}^2}$ is centered while the ZP-element is not. The technical report [18] details the non-trivial but algorithmic derivation of $\lambda_{M_{\mathbb{Z}^2}} f$ and other quasi-interpolant functionals in this paper according to [11, (III.19)].

For a discrete input $f : \mathbb{Z}^2 \to \mathbb{R}$, we can approximate the directional derivatives by finite differences with 8 neighbors (see Figure 5 for the stencil)

$$\lambda_{\mathbb{Z}^2}(f(\cdot+\boldsymbol{j})) \approx \frac{4}{3}f(\boldsymbol{j}) - \frac{1}{24}\sum_{\boldsymbol{\xi}\in\boldsymbol{\Xi}_{\mathrm{ZP}}}(f(\boldsymbol{j}+\boldsymbol{\xi}) + f(\boldsymbol{j}-\boldsymbol{\xi})).$$

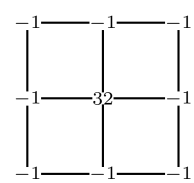

Figure 5. Quasi-interpolation stencil of $M_{\mathbb{Z}^2}$ (scaled by 24).

The 7-Direction Trivariate Box-Spline. In dimension three, $\boldsymbol{\Xi}_{\mathbb{Z}^3}$ is the direction matrix of the 7-*direction trivariate box-spline* [4, 5, 19, 20] $M_{\mathbb{Z}^3}$:

$$\boldsymbol{\Xi}_{\mathbb{Z}^3} := \begin{bmatrix} 1 & 0 & 0 & 1 & -1 & 1 & -1 \\ 0 & 1 & 0 & 1 & 1 & -1 & -1 \\ 0 & 0 & 1 & 1 & 1 & 1 & 1 \end{bmatrix}.$$

The (total) degree of $M_{\mathbb{Z}^3}$ is $2^{3-1} = 4$ and $M_{\mathbb{Z}^3} \in C^{2^{3-2}} = C^2$. The same continuity is achieved by the tri-cubic B-spline of total degree $12 - 3 = 9$. Kim and Peters [20] derived the BB-net of $M_{\mathbb{Z}^3}$.

A quasi-interpolant $Q_{\mathbb{Z}^3}$ (see (5)) with optimal approximation order 4 for the spline space $S_{\mathbb{Z}^3} := \operatorname{span}\left(M_{\mathbb{Z}^3}(\cdot - \boldsymbol{j})\right)_{\boldsymbol{j}\in\mathbb{Z}^3}$ is (cf. [18])

$$\begin{aligned}\lambda_{\mathbb{Z}^3} f :=& (f - \frac{5}{24}(D_1^2 + D_2^2 + D_3^2)f)(\mathbf{0}) \\ =& (f - \frac{1}{24}(D_1^2 + D_2^2 + D_3^2 + (D_1 + D_2 + D_3)^2 + (-D_1 + D_2 + D_3)^2 \\ &+ (D_1 - D_2 + D_3)^2 + (-D_1 - D_2 + D_3)^2))(\mathbf{0}) \\ =& (f - \frac{1}{24}\sum_{\boldsymbol{\xi}\in\boldsymbol{\Xi}_{\mathbb{Z}^3}} D_{\boldsymbol{\xi}}^2 f)(\mathbf{0}).\end{aligned} \tag{6}$$

For discrete data $f : \mathbb{Z}^3 \to \mathbb{R}$, we can approximate the directional derivatives by finite differences with 14 neighbors

$$\lambda_{\mathbb{Z}^3}\left(f(\cdot + \boldsymbol{j})\right) \approx \frac{19}{12} f(\boldsymbol{j}) - \frac{1}{24}\sum_{\boldsymbol{\xi}\in\boldsymbol{\Xi}_{\mathbb{Z}^3}} f(\boldsymbol{j} + \boldsymbol{\xi}) + f(\boldsymbol{j} - \boldsymbol{\xi}), \quad \boldsymbol{j}\in\mathbb{Z}^3.$$

Alternatively, we can approximate (6) using 6 neighbors as

$$\lambda_{\mathbb{Z}^3}\left(f(\cdot + \boldsymbol{j})\right) \approx \frac{9}{4} f(\boldsymbol{j}) - \frac{5}{24}\sum_{i=1}^{3}(f(\boldsymbol{j} + \mathbf{e}_n^i) + f(\boldsymbol{j} - \mathbf{e}_n^i)), \quad \boldsymbol{j}\in\mathbb{Z}^3.$$

4. Box-splines on Non-Cartesian Lattices

We leverage that, given an invertible linear map $\mathbf{L}$ on $\mathbb{R}^n$, [11, (I.23)]

$$M_{\boldsymbol{\Xi}} = |\det \mathbf{L}| M_{\mathbf{L}\boldsymbol{\Xi}} \circ \mathbf{L}.$$

Hence, given a square generator matrix $\mathbf{G}$, any weighted sum of the shifts of the (scaled) box-spline

$$\widetilde{M}_{\boldsymbol{\Xi}} := |\det \mathbf{G}| M_{\mathbf{G}\boldsymbol{\Xi}}$$

on the possibly non-Cartesian lattice $\mathbf{G}\mathbb{Z}^n$ can be expressed as a weighted sum of the shifts of $M_{\boldsymbol{\Xi}}$ on the Cartesian lattice $\mathbb{Z}^n$ by *change of variables*:

$$\sum_{\boldsymbol{j}\in\mathbf{G}\mathbb{Z}^n} \widetilde{M}_{\boldsymbol{\Xi}}(\cdot - \boldsymbol{j}) a(\boldsymbol{j}) = \sum_{\boldsymbol{k}\in\mathbb{Z}^n} M_{\boldsymbol{\Xi}}(\mathbf{G}^{-1}\cdot - \boldsymbol{k}) a(\mathbf{G}\boldsymbol{k}) \tag{7}$$

where $a : \mathbf{G}\mathbb{Z}^n \to \mathbb{R}$ is a mesh function (the spline coefficients) on $\mathbf{G}\mathbb{Z}^n$. In the bivariate setting (7) was used by de Boor and Höllig [21, page 650]. We denote the spline space spanned by the shifts of $\widetilde{M}_{\boldsymbol{\Xi}}$ on $\mathbf{G}\mathbb{Z}^n$ by

$$S_{\boldsymbol{\Xi}}^{\mathbf{G}} := \operatorname{span}\left(\widetilde{M}_{\boldsymbol{\Xi}}(\cdot - \boldsymbol{j})\right)_{\boldsymbol{j}\in\mathbf{G}\mathbb{Z}^n}.$$

By omitting $\mathbf{G} = \mathbf{I}_n$, we define $S_{\boldsymbol{\Xi}} := S_{\boldsymbol{\Xi}}^{\mathbf{I}_n}$.

By (7), the sequence $\left(\widetilde{M}_{\boldsymbol{\Xi}}(\cdot - \boldsymbol{j})\right)_{\boldsymbol{j}\in\mathbf{G}\mathbb{Z}^n}$ is linearly independent if and only if $\boldsymbol{\Xi}$ is unimodular. We will leverage a general theorem on quasi-interpolation whose proof appeared in [9].

Lemma 2 (Quasi-interpolation; [9]). *Let* $\boldsymbol{\alpha} \in \mathbb{Z}_+^n$ *be a* multi-index*,* D_j *the directional derivative along* $\mathbf{e}_n^j$ *and* $D_{\mathbf{G}}^{\boldsymbol{\alpha}} := \prod_{\boldsymbol{v}\in\mathbf{G}} D_{\boldsymbol{v}}^{\boldsymbol{\alpha}_{\boldsymbol{v}}}$ *(with* $\boldsymbol{\alpha}_{\boldsymbol{v}}$ *denoting the entry of* $\boldsymbol{\alpha}$ *corresponding to* $\boldsymbol{v}$*) a composition of directional derivatives* $D_{\boldsymbol{v}} := \sum_{j=1}^n \boldsymbol{v}(j) D_j$ *along the columns of* $\mathbf{G}$*. Let further* $\{g_{\boldsymbol{\alpha}}\}$ *be the Appell sequence given in [11, (III.19)] and define the linear functional (cf. [11, (III.22)])*

$$\lambda_{M_{\Xi}} f := \sum_{|\boldsymbol{\alpha}|\leq m(\Xi)} g_{\boldsymbol{\alpha}}(\mathbf{0}) \left(D^{\boldsymbol{\alpha}} f\right)(\mathbf{0}).$$

The quasi-interpolant $Q_{M_{\Xi}}^{\mathbf{G}}$ *for* $S_{\Xi}^{\mathbf{G}}$ *defined by the functional*

$$\begin{aligned}\lambda_{M_{\Xi}}^{\mathbf{G}}\left(f\left(\cdot+\boldsymbol{j}\right)\right) &:= \lambda_{M_{\Xi}}\left(\left(f\circ\mathbf{G}\right)\left(\cdot+\mathbf{G}^{-1}\boldsymbol{j}\right)\right)\\ &= \sum_{|\boldsymbol{\alpha}|\leq m(\Xi)} g_{\boldsymbol{\alpha}}(\mathbf{0}) \left(D_{\mathbf{G}}^{\boldsymbol{\alpha}} f\right)(\boldsymbol{j}), \quad \boldsymbol{j}\in\mathbf{G}\mathbb{Z}^n,\end{aligned}$$

provides the same maximal approximation order $m(\Xi)+1$ *(i.e. reproduces all Taylor terms up to degree* $m(\Xi)$*) as does* $Q_{M_{\Xi}}$ *defined by* $\lambda_{M_{\Xi}}$ *for* S_{Ξ}*.*

We can now investigate the major non-Cartesian root lattices and corresponding symmetric box-splines.

5. The Symmetric $n(n+1)/2$-direction Box-Spline on the $\mathcal{A}_n$ Lattice

On the $\mathcal{A}_n$ lattice, we construct a symmetric box-spline[1] $M_{\mathcal{A}_n}^{\pm}$ (15) by convolving in the directions of the root system $\mathscr{A}_n$ (8). These are the directions to a lattice point's $n(n+1)$ nearest lattice neighbors on the $\mathcal{A}_n$ lattice (see Figure 8(b) for the trivariate case and the examples in Section 5.2). Since the $\mathcal{A}_n$ lattice is usually defined as embedded in $H_{\mathbf{j}}^n \subsetneq \mathbb{R}^{n+1}$ [10], the key to this construction is to embed it in $\mathbb{R}^n$, one-to-one between $H_{\mathbf{j}}^n$ and $\mathbb{R}^n$, with the help of a pair of orthogonal matrices $\mathbf{X}_n^{\pm}$ (9) of size $n\times(n+1)$. Geometrically, an equivalent basis for the $\mathcal{A}_n$ lattice can also be constructed by taking the n edges sharing a vertex of an n-dimensional equilateral simplex. In dimension two, either construction results in the well-known 3-direction linear box-spline on the hexagonal lattice. In dimension three, it yields the 6-direction box-spline on the FCC lattice (Section 5.2) proposed by Entezari [7].

5.1. Lattice, Definition and Properties

The Root system $\mathscr{A}_n$. The finite reflection group $\mathscr{A}_n$ is composed of n hyperplanes with their dihedral angles described by the Coxeter diagram in Table 2. It can be formulated by the root system embedded in $\mathbb{R}^{n+1}$ with Cartesian coordinates as follows [10, 22]:

$$\mathscr{A}_n = \left\{\pm(\mathbf{e}_{n+1}^i - \mathbf{e}_{n+1}^j) : 1\leq i\neq j\leq n+1\right\}. \tag{8}$$

[1] Although, formally, the $\pm$ superscript indicates a pair of box-splines, we will in the following refer to it as a singleton, assuming a choice has been made.

In general, we can obtain n-dimensional roots of $\mathscr{A}_n$ by any orthogonal transformation that maps $H^n_{\mathbf{j}}$ to $\mathbb{R}^n$. A pair of such matrices are

$$\mathbf{X}_n^{\pm} := (\mathbf{A}_{\mathrm{P}}^*(\mathbf{A}_n^{*\pm})^{-1})^t = \mathbf{A}_n^{\pm}\mathbf{A}_{\mathrm{P}}^{*\,t} = \mathbf{A}_n^{*\pm}\begin{bmatrix} \mathbf{I}_n & -\mathbf{j}_n \end{bmatrix} : H^n_{\mathbf{j}} \to \mathbb{R}^n \tag{9}$$

where [23]

$$\mathbf{A}_{\mathrm{P}}^* := \frac{1}{n+1}\begin{bmatrix} (n+1)\mathbf{I}_n - \mathbf{J}_n \\ -\mathbf{j}_n^t \end{bmatrix}, \tag{10}$$

$$\mathbf{A}_n^{\pm} := \mathbf{I}_n + \frac{1}{n}\left(-1 \pm \sqrt{n+1}\right)\mathbf{J}_n \tag{11}$$

and

$$\mathbf{A}_n^{*\pm} := \mathbf{I}_n + \frac{1}{n}\left(-1 \pm \frac{1}{\sqrt{n+1}}\right)\mathbf{J}_n. \tag{12}$$

Note that, while

$$(\mathbf{X}_n^{\pm})^t\mathbf{X}_n^{\pm} = \mathbf{I}_{n+1} - \frac{1}{n+1}\mathbf{J}_{n+1} \neq \mathbf{I}_{n+1}, \tag{13}$$

$\mathbf{X}_n^{\pm}$ are orthogonal transformations that preserve lengths and angles, since $\mathbf{J}_{n+1}\boldsymbol{x} = \mathbf{0}_{n+1}$ for $\boldsymbol{x} \in H^n_{\mathbf{j}}$ and hence

$$(\mathbf{X}_n^{\pm}\boldsymbol{x}) \cdot (\mathbf{X}_n^{\pm}\boldsymbol{x}) = \boldsymbol{x} \cdot \boldsymbol{x}.$$

The symmetry group of $\mathscr{A}_n$ consists of the symmetric group of all $(n+1)!$ permutations of its coordinates and the group of changing the sign of all the coordinates, hence its order is $(n+1)!2$ [10]. In dimension two, this follows from the 12-fold symmetry of the hexagon.

The Root lattice $\mathcal{A}_n$. The root lattice $\mathcal{A}_n$ is generated by all the integer linear combinations of the roots of $\mathscr{A}_n$. A generator matrix for the $\mathcal{A}_n$ lattice is $\mathbf{A}_{\mathrm{P}} := [\mathbf{I}_n - \mathbf{j}_n]^t \in \mathbb{R}^{(n+1)\times n}$. $\mathcal{A}_n$ can be either embedded in $H^n_{\mathbf{j}} \subsetneq \mathbb{R}^{n+1}$ [10, page 109] or directly in $\mathbb{R}^n$ using the square generator matrix $\mathbf{A}_n^{\pm}$ obtained by applying $\mathbf{X}_n^{\pm}$ to $\mathbf{A}_{\mathrm{P}}$:

$$\mathbf{X}_n^{\pm}\mathbf{A}_{\mathrm{P}} = \mathbf{A}_n^{\pm}\mathbf{A}_{\mathrm{P}}^{*\,t}\mathbf{A}_{\mathrm{P}} = \mathbf{A}_n^{\pm}.$$

In low dimensions, $\mathcal{A}_2 \cong \mathcal{A}_2^*$ is equivalent to the hexagonal lattice and $\mathcal{A}_3 \cong \mathcal{D}_3$ is equivalent to the FCC lattice.

The Box-spline $M^{\pm}_{\mathcal{A}_n}$. The $n(n+1)/2$-direction box-spline on the $\mathcal{A}_n$ lattice is defined by the non-parallel directions of $\mathscr{A}_n$ transformed by $\mathbf{X}_n^{\pm}$:

$$\boldsymbol{\Xi}^{\pm}_{\mathcal{A}_n} := \bigcup_{1\le i<j\le n+1}\{\mathbf{X}_n^{\pm}(\mathbf{e}^i_{n+1} - \mathbf{e}^j_{n+1})\} \tag{14}$$

and the 'centered' and 're-normalized' box-spline is defined as

$$M^{\pm}_{\mathcal{A}_n} := |\det \mathbf{A}_n^{\pm}| M_{\boldsymbol{\Xi}^{\pm}_{\mathcal{A}_n}}(\cdot + \sum_{\boldsymbol{\xi}\in\boldsymbol{\Xi}^{\pm}_{\mathcal{A}_n}} \boldsymbol{\xi}/2). \tag{15}$$

The following lemma will be helpful to prove the properties of $M^{\pm}_{\mathcal{A}_n}$.

Lemma 3. *Let $\Xi^{\perp \boldsymbol{v}} := \{\boldsymbol{\xi} \in \Xi : \boldsymbol{\xi} \cdot \boldsymbol{v} = 0\}$ be the vectors in Ξ orthogonal to $\boldsymbol{v} \neq \mathbf{0}$. Then*

$$\max_{\boldsymbol{v}\in\mathbb{R}^n} \#(\Xi^{\pm}_{\mathcal{A}_n})^{\perp \boldsymbol{v}} = \binom{n}{2}.$$

Proof. We observe that, since $\mathbf{X}^{\pm}_n$ maps $H^n_{\mathbf{j}}$ one-to-one onto $\mathbb{R}^n$,

$$\max_{\boldsymbol{v}\in\mathbb{R}^n} \#(\Xi^{\pm}_{\mathcal{A}_n})^{\perp \boldsymbol{v}} = \max_{\boldsymbol{\omega}\in H^n_{\mathbf{j}}\subsetneq\mathbb{R}^{n+1}} \#\Xi^{\perp\boldsymbol{\omega}}, \quad \text{where} \quad \Xi := \bigcup_{1\le i<j\le n+1} \{\mathbf{e}^i_{n+1} - \mathbf{e}^j_{n+1}\}.$$

If we set $\boldsymbol{\omega} := [\,{}^{\mathbf{j}_n}_{-n}\,] \in H^n_{\mathbf{j}}$ then $\boldsymbol{\omega}\cdot(\mathbf{e}^i_{n+1} - \mathbf{e}^j_{n+1}) = 0$ exactly when $0 \le i < j \le n$, i.e. $\#\Xi^{\perp\boldsymbol{\omega}} = \binom{n}{2}$. To show that $\binom{n}{2}$ is also an upper bound, Let k be the maximum number of nonzero identical entries in $\boldsymbol{\omega}$. Without loss of generality, these are the first k entries and these entries are 1. Since $\boldsymbol{\omega} \in H^n_{\mathbf{j}}$, i.e. $\boldsymbol{\omega}\cdot\mathbf{j}_{n+1} = 0$, $k < n+1$. To show that the number of vectors in Ξ orthogonal to $\boldsymbol{\omega}$ is maximized for $k = n$, we split $\Xi := \mathbf{Z}_1 \sqcup \mathbf{Z}_2 \sqcup \mathbf{Z}_3$,

$$\begin{aligned}
\mathbf{Z}_1 &:= \{\mathbf{e}^i_{n+1} - \mathbf{e}^j_{n+1} : 1 \le i < j \le k\},\\
\mathbf{Z}_2 &:= \{\mathbf{e}^i_{n+1} - \mathbf{e}^j_{n+1} : 1 \le i \le k, k+1 \le j \le n+1\},\\
\mathbf{Z}_3 &:= \{\mathbf{e}^i_{n+1} - \mathbf{e}^j_{n+1} : k+1 \le i < j \le n+1\}.
\end{aligned}$$

Since for all $\boldsymbol{\zeta}_2 \in \mathbf{Z}_2$, $\boldsymbol{\zeta}_2\cdot\boldsymbol{\omega} = 1 - \boldsymbol{\omega}(j) \neq 0$, we have $\mathbf{Z}_2^{\perp\boldsymbol{\omega}} = \emptyset$. Also $\binom{k}{2} = \#\mathbf{Z}_1 \ge \#\mathbf{Z}_1^{\perp\boldsymbol{\omega}}$ and $\binom{n-k+1}{2} = \#\mathbf{Z}_3 \ge \#\mathbf{Z}_3^{\perp\boldsymbol{\omega}}$, so that

$$\begin{aligned}
\#\Xi^{\perp\boldsymbol{\omega}} &= \#\mathbf{Z}_1^{\perp\boldsymbol{\omega}} + \#\mathbf{Z}_3^{\perp\boldsymbol{\omega}} \le \binom{k}{2} + \binom{n-k+1}{2}\\
&= \frac{n^2-n}{2} + k^2 - k - kn + n = \binom{n}{2} + (k-n)(k-1) \le \binom{n}{2}
\end{aligned}$$

since $(k-n)(k-1) \le 0$ for $1 \le k < n+1$. $\square$

Theorem 2 (Properties of $M^{\pm}_{\mathcal{A}_n}$)**.** *The box-spline $M^{\pm}_{\mathcal{A}_n}$ has (i) polynomial degree $n(n-1)/2$, (ii) $M^{\pm}_{\mathcal{A}_n} \in C^{n-2}$ and (iii) the sequence $\big(M^{\pm}_{\mathcal{A}_n}(\cdot - \boldsymbol{j})\big)_{\boldsymbol{j}\in\mathbf{A}^{\pm}_n\mathbb{Z}^n}$ is linearly independent.*

Proof. (i) The degree follows from $\#\Xi_{\mathcal{A}_n} - n = n(n+1)/2 - n = n(n-1)/2$.

(ii) By Lemma 3, the maximal number of columns of $\Xi^{\pm}_{\mathcal{A}_n}$ lying in a hyperplane is $\binom{n}{2}$. Therefore $m(\Xi^{\pm}_{\mathcal{A}_n}) = (n(n+1)/2 - n(n-1)/2) - 1 = n-1$ and $M^{\pm}_{\mathcal{A}_n} \in C^{n-2}$.

(iii) Since $M^{\pm}_{\mathcal{A}_n}$ is shifted on $\mathbf{A}^{\pm}_n\mathbb{Z}^n \cong \mathcal{A}_n$, the sequence $\big(M^{\pm}_{\mathcal{A}_n}(\cdot - \boldsymbol{j})\big)_{\boldsymbol{j}\in\mathbf{A}^{\pm}_n\mathbb{Z}^n}$ is linearly independent if and only if $\Xi_n := (\mathbf{A}^{\pm}_n)^{-1}\Xi^{\pm}_{\mathcal{A}_n}$ is unimodular. By the second equality in (9), for each column of Ξ_n, i.e. for $1 \le i < j \le n+1$,

$$(\mathbf{A}^{\pm}_n)^{-1}\mathbf{X}^{\pm}_n(\mathbf{e}^i_{n+1} - \mathbf{e}^j_{n+1}) = \mathbf{A}^{*\,t}_{\mathrm{P}}(\mathbf{e}^i_{n+1} - \mathbf{e}^j_{n+1}) = \begin{cases} \mathbf{e}^i_n, & j = n+1\\ \mathbf{e}^i_n - \mathbf{e}^j_n, & j < n+1 \end{cases}$$

and therefore $\Xi_n = \mathbf{I}_n \cup \bigcup_{1\le i<j\le n}\{\mathbf{e}^i_n - \mathbf{e}^j_n\}$. Since $\boldsymbol{\xi}\cdot\mathbf{j}_n = 0$ for $\boldsymbol{\xi} \in \Xi^{\pm}_{\mathcal{A}_n}\backslash\mathbf{I}_n$, we need only consider square sub-matrices (basis matrices) $\mathbf{Z}_n$ of Ξ_n that contain at least one unit vector. (Otherwise the

determinant of the square sub-matrix is zero and this is compatible with unimodularity.) Now pick any $\mathbf{Z}_n$ of full rank with column $\mathbf{e}_n^i$ for some $1 \le i \le n$. Let $\mathbf{Z}_{n-1}$ be its submatrix obtained by removing the column $\mathbf{e}_n^i$ and row i and flipping the sign of any column that has a single -1 entry. Then $|\det \mathbf{Z}_n| = |\det \mathbf{Z}_{n-1}|$. If, for some j, both $\mathbf{e}_n^j$ and $\mathbf{e}_n^i - \mathbf{e}_n^j$ had been columns in $\mathbf{Z}_{n-1}$, then $\det \mathbf{Z}_{n-1} = 0$ and this cannot be since $\mathbf{Z}_n$ was chosen of full rank. Therefore $\mathbf{Z}_{n-1} \subset \mathbf{\Xi}_{n-1}$ and we can now repeat the above determinant reduction until we read off that $\mathbf{\Xi}_2 := \left[\begin{smallmatrix} 1 & 0 & 1 \\ 0 & 1 & -1 \end{smallmatrix}\right]$ is unimodular. Therefore $\mathbf{\Xi}_n$ is unimodular as claimed.

$\square$

5.2. Examples

The 3-Direction Bivariate Box-Spline on the Hexagonal Lattice. In dimension two, we get the direction matrix $\mathbf{\Xi}^{\pm}_{\mathcal{A}_2}$ (14) and the generator matrix $\mathbf{A}_2^{\pm}$ (11)

$$\mathbf{\Xi}^{\pm}_{\mathcal{A}_2} := \mathbf{X}_2^{\pm} \begin{bmatrix} 1 & 1 & 0 \\ -1 & 0 & 1 \\ 0 & -1 & -1 \end{bmatrix} = \frac{1}{2} \begin{bmatrix} 2 & 1 \pm \sqrt{3} & -1 \pm \sqrt{3} \\ -2 & -1 \pm \sqrt{3} & 1 \pm \sqrt{3} \end{bmatrix}, \qquad \mathbf{A}_2^{\pm} := \frac{1}{2} \begin{bmatrix} 1 \pm \sqrt{3} & -1 \pm \sqrt{3} \\ -1 \pm \sqrt{3} & 1 \pm \sqrt{3} \end{bmatrix}.$$

The box-spline $M^{\pm}_{\mathcal{A}_2}$ defined by $\mathbf{\Xi}^{\pm}_{\mathcal{A}_2}$ and $\mathbf{A}_2^{\pm}$ is equivalent to the 3-direction linear box-spline on the hexagonal lattice.

The 6-direction box-spline on the FCC lattice. In dimension three, we get the direction matrices (14)

$$\mathbf{\Xi}^{+}_{\mathcal{A}_3} = \frac{1}{3} \begin{bmatrix} 3 & 3 & 4 & 0 & 1 & 1 \\ -3 & 0 & 1 & 3 & 4 & 1 \\ 0 & -3 & 1 & -3 & 1 & 4 \end{bmatrix}, \quad \mathbf{\Xi}^{-}_{\mathcal{A}_3} = \begin{bmatrix} 1 & 1 & 0 & 0 & -1 & -1 \\ -1 & 0 & -1 & 1 & 0 & -1 \\ 0 & -1 & -1 & -1 & -1 & 0 \end{bmatrix}$$

and by (11), the generator matrices for the FCC ($\cong \mathcal{A}_3$) lattice,

$$\mathbf{A}_3^{+} := \frac{1}{3} \begin{bmatrix} 4 & 1 & 1 \\ 1 & 4 & 1 \\ 1 & 1 & 4 \end{bmatrix}, \quad \mathbf{A}_3^{-} := - \begin{bmatrix} 0 & 1 & 1 \\ 1 & 0 & 1 \\ 1 & 1 & 0 \end{bmatrix}$$

This is equivalent to the 6-direction box-spline on the FCC lattice [7, 8]. Figure 8(b) shows the directions and support of $M^{-}_{\mathcal{A}_3}$. According to [8], a quasi-interpolant of $M^{\pm}_{\mathcal{A}_3}$ that provides the maximal approximation order $m(\mathbf{\Xi}^{\pm}_{\mathcal{A}_3}) + 1 = 3$ is defined by the functional

$$\lambda^{\mathbf{A}_3^{\pm}}_{\mathbf{\Xi}^{\pm}_{\mathcal{A}_3}}(f(\cdot + \boldsymbol{j})) := (f - \frac{1}{24} \sum_{\boldsymbol{\xi} \in \mathbf{\Xi}^{\pm}_{\mathcal{A}_3}} D^2_{\boldsymbol{\xi}} f)(\boldsymbol{j}), \quad \boldsymbol{j} \in \mathbf{A}_3^{\pm} \mathbb{Z}^n.$$

6. Symmetric $(n+1)$-direction Box-Spline on the $\mathcal{A}_n^*$ Lattice

The members of the family M_r [23] of n-variate box-splines are defined by r-fold convolution, in the n directions of the Cartesian lattice plus a diagonal and generalize the 'hat' functions. The box-splines are popular due to the linear independence of their Cartesian shifts and approximation properties. But the footprints of the box-splines are asymmetrically distorted in the diagonal direction (see e.g. Figure 4(b)). To make reconstruction of fields less biased, convolution and shifts on 2- and 3-dimensional non-Cartesian lattices, the hexagonal lattice and the BCC lattice respectively, have recently been advocated [3, 6].

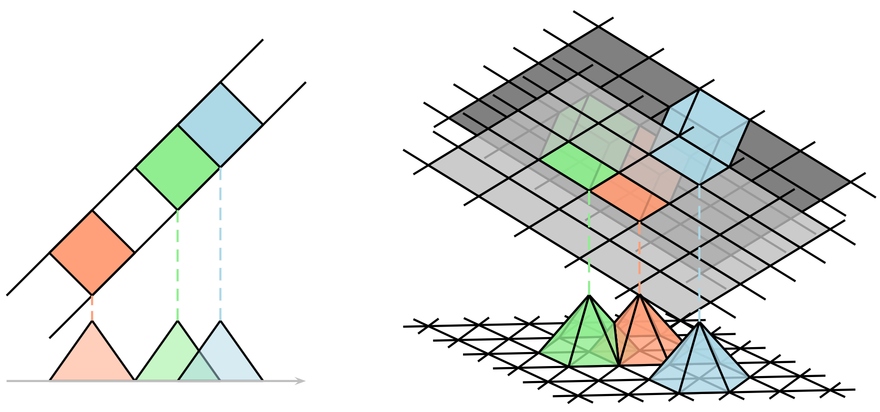

(a) $n = 1$

(b) $n = 2$

Figure 6. Orthogonal projection of unit cubes along the diagonal direction for (a) $n = 1$ and (b) $n = 2$. [23]

Kim and Peters [23] generalized bivariate box-splines on the hexagonal lattice and trivariate box-splines on the BCC lattice to symmetric n-variate box-splines $M_r^{*\pm}$ defined by the directions connecting to the $2(n+1)$ nearest neighbors of the $\mathcal{A}_n^*$ lattice (see e.g. Figure 8(c) for $n = 3$). By defining the $\mathcal{A}_n^*$ lattice directly in $\mathbb{R}^n$, as we did for the $\mathcal{A}_n$ lattice, the geometric construction of the shifts of the symmetric linear box-spline $M_1^{*\pm}$ on the $\mathcal{A}_n^*$ lattice simplifies to the classical construction of n-variate box-splines by projection: The shifts of the symmetric linear box-spline on $\mathcal{A}_n^*$ are the *orthogonal* projection of a slab of thickness 1, decomposed into unit cubes, along the diagonal of the cubes (Figure 6). By comparison, M_1 has the same preimage, but its support is distorted by its anisotropic direction matrix. Kim and Peters [23] documented the support, its partition, the desirable properties shared with M_r and, for the important case $r = 2$, the quasi-interpolant construction associated with $M_2^{*\pm}$ in *any* number of variables n.

6.1. Lattice, Definition and Properties

The Root lattice $\mathcal{A}_n^*$. As in the case of the $\mathcal{A}_n$ lattice, Kim and Peters [23] used a geometric construction of $\mathcal{A}_n^*$ in $\mathbb{R}^n$ to obtain pairs of square generator matrices $\mathbf{A}_n^{*\pm}$ shown in Table 2, for the $\mathcal{A}_n^*$ lattice. We note that $\mathcal{A}_2^* \cong \mathcal{A}_2$ is equivalent to the hexagonal lattice and $\mathcal{A}_3^* \cong \mathcal{D}_3^*$ is equivalent to the BCC lattice. For each case, examples of generator matrices (12) are, for $n = 2$,

$$\mathbf{A}_2^{*\pm} := \frac{1}{2}\begin{bmatrix} 1 \pm 1/\sqrt{3} & -1 \pm 1/\sqrt{3} \\ -1 \pm 1/\sqrt{3} & 1 \pm 1/\sqrt{3} \end{bmatrix}$$

and for $n = 3$,

$$\mathbf{A}_3^{*+} := \frac{1}{6}\begin{bmatrix} 5 & -1 & -1 \\ -1 & 5 & -1 \\ -1 & -1 & 5 \end{bmatrix} \quad \text{and} \quad \mathbf{A}_3^{*-} := \frac{1}{2}\begin{bmatrix} 1 & -1 & -1 \\ -1 & 1 & -1 \\ -1 & -1 & 1 \end{bmatrix}.$$

$\mathcal{A}_n^*$ is the optimal sampling lattice in dimensions two and three [7, 24, 25]. In higher dimensions, Figure 1 shows that $\mathcal{A}_n$ packs spheres better than the Cartesian lattice, making $\mathcal{A}_n^*$ a better sampling lattice than $\mathbb{Z}^n$.

The Box-spline $M_{\mathcal{A}_n^*}^{\pm}$. On the lattice (10) $\mathbf{A}_{\mathrm{P}}^*\mathbb{Z}^n \cong \mathcal{A}_n^*$ embedded in $\mathbb{R}^{n+1}$, there are $2(n+1)$ lattice points nearest the origin. [10] Their Cartesian coordinates are

$$\{\pm(\mathbf{e}_{n+1}^j - \frac{1}{n+1}\mathbf{j}_{n+1}) \in H_{\mathbf{j}}^n : 1 \leq j \leq n+1\}. \tag{16}$$

The $(n+1)$-direction box-spline $M_{\mathcal{A}_n^*}^{\pm}$ on the $\mathcal{A}_n^*$ lattice is constructed by the directions to the $2(n+1)$ nearest lattice points. As in Section 5, we transform the directions of (16) to $\mathbb{R}^n$ by $\mathbf{X}_n^{\pm}$:

$$\begin{aligned}\mathbf{T}_1^{*\pm} &:= \mathbf{X}_n^{\pm}\left(\mathbf{I}_{n+1} - \frac{1}{n+1}\mathbf{J}_{n+1}\right) = \mathbf{A}_n^{*\pm}\begin{bmatrix} \mathbf{I}_n & -\mathbf{j}_n \end{bmatrix}\begin{bmatrix} \mathbf{I}_n - \mathbf{J}_n/(n+1) & -\mathbf{j}_n/(n+1) \\ -\mathbf{j}_n^t/(n+1) & n/(n+1) \end{bmatrix} \\ &= \mathbf{A}_n^{*\pm}\begin{bmatrix} \mathbf{I}_n & -\mathbf{j}_n \end{bmatrix} =: \mathbf{A}_n^{*\pm}\mathbf{T}_1.\end{aligned}$$

With the square generator matrix $\mathbf{A}_n^{*\pm}$, the $(n+1)$-direction (linear) box-spline on the $\mathcal{A}_n^*$ lattice is defined as

$$M_{\mathcal{A}_n^*}^{\pm} := M_1^{*\pm} := |\det \mathbf{A}_n^{*\pm}| M_{\mathbf{T}_1^{*\pm}}(\cdot + \sum_{\boldsymbol{\xi}\in\mathbf{T}_1^{*\pm}} \boldsymbol{\xi}/2) = |\det \mathbf{A}_n^{*\pm}| M_{\mathbf{T}_1^{*\pm}}.$$

The properties of $M_{\mathcal{A}_n^*}^{\pm}$ were already established in [23] and are listed for completeness.

Theorem 3 (Properties of $M_{\mathcal{A}_n^*}^{\pm}$; [23])**.** *The box-spline $M_{\mathcal{A}_n^*}^{\pm}$ has The polynomial degree 1, $M_{\mathcal{A}_n^*}^{\pm} \in C^0$ and the sequence $\left(M_{\mathcal{A}_n^*}^{\pm}(\cdot - \boldsymbol{j})\right)_{\boldsymbol{j}\in\mathbf{A}_n^*\mathbb{Z}^n}$ is linearly independent.*

The family of box-splines $M_r^{*\pm}$ constructed by the r-fold repetition of $\mathbf{T}_1^{*\pm}$, $\mathbf{T}_r^{*\pm} := \bigcup_{j=1}^r \mathbf{T}_1^{*\pm}$, was investigated in [23]. We restate the main result on quasi-interpolants for $r = 2$: The quasi-interpolant of $M_2^{*\pm}$, defined by the functional

$$\lambda_2^{*\pm}(f(\cdot + \boldsymbol{j})) := \lambda_{\mathbf{T}_2}^{\mathbf{A}_n^{*\pm}}(f(\cdot + \boldsymbol{j})) := \left(f - \frac{1}{12}\sum_{\boldsymbol{\xi}\in\mathbf{T}_1^{*\pm}} D_{\boldsymbol{\xi}}^2 f\right)(\boldsymbol{j}), \quad \boldsymbol{j} \in \mathbf{A}_n^{*\pm}\mathbb{Z}^n$$

provides the maximal approximation order $m(\mathbf{T}_2^{*\pm}) + 1 = 4$.

Examples of symmetric box-splines on the $\mathcal{A}_n^*$ lattice can be found in [23].

7. Symmetric $n(n-1)$-direction Box-Spline on the $\mathcal{D}_n$ Lattice

For $n \geq 3$, the root lattice $\mathcal{D}_n$ can be viewed as a sub-lattice of the integer grid (Cartesian lattice), namely all integer points whose sum is even [10]. The box-spline $M_{\mathcal{D}_n}$ is constructed by the directions of the root system $\mathscr{D}_n$. In $\mathbb{R}^3$, this (also) yields the 6-direction box-spline on the FCC lattice [7]. (See Section 5.2.)

7.1. Lattice, Definition and Properties

The Root system $\mathscr{D}_n$. The root system $\mathscr{D}_n$ can be described by the Coxeter diagram in Table 2. There it is composed of all $\#\mathscr{D}_n = 2n(n-1)$ integer vectors of length $\sqrt{2}$, i.e., [10, 22]

$$\mathscr{D}_n = \left\{ \pm \mathbf{e}_n^i \pm \mathbf{e}_n^j : 1 \leq i \neq j \leq n \right\}. \tag{17}$$

Due to the three rightmost mandatory nodes of the Coxeter diagram for $\mathscr{D}_n$ (Table 2), $\mathscr{D}_n$ is only defined for $n \geq 3$; and in dimension three, $\mathscr{D}_3 \cong \mathscr{A}_3$.

The Root lattice $\mathcal{D}_n$. The root lattice $\mathcal{D}_n$ is generated by all integer linear combinations of the roots of $\mathscr{D}_n$. Alternatively, $\mathcal{D}_n$ is defined as all integer points of $\mathbb{Z}^n$ where the sum of their elements is always even when $\mathscr{D}_n$ is formulated as (17) [10]:

$$\mathcal{D}_n := \{ \boldsymbol{i} \in \mathbb{Z}^n : \boldsymbol{i} \cdot \mathbf{j}_n \text{ is even} \}.$$

A set of simple roots associated with the Coxeter diagram in Table 2, [22]

$$\mathbf{G}_{\mathcal{D}_n} := \left\{ -\mathbf{e}_n^{n-1} - \mathbf{e}_n^n \right\} \cup \bigcup_{j=1}^{n-1} \left\{ \mathbf{e}_n^i - \mathbf{e}_n^n \right\} = \begin{bmatrix} 1 & & & & \\ & 1 & & & \\ & & \ddots & & \\ & & & 1 & -1 \\ -1 & -1 & \cdots & -1 & -1 \end{bmatrix} = \begin{bmatrix} \mathbf{I}_{n-1} & -\mathbf{e}_{n-1}^{n-1} \\ -\mathbf{j}_{n-1}^t & -1 \end{bmatrix}$$

serves as a square generator matrix for the $\mathcal{D}_n$ lattice. For $n \neq 4$, the order is $n!2^n$ since the symmetry group of $\mathcal{D}_n$ consists of all $n!$ permutations of coordinates, 2^{n-1} sign changes of even-sum coordinates and 2 sign changes of the last coordinates. For $n = 4$, the symmetry group is that of the 24-*cell* [10, 26]. Besides the symmetries of the first two bullets above, it consists of the 3! permutations of three roots according to the symmetry of its Coxeter diagram (Figure 7). Hence the total order of $\mathcal{D}_4$ is $4! \times 2^3 \times 3! = 1152$.

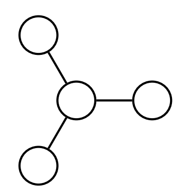

Figure 7. Coxeter diagram of the root system $\mathscr{D}_4$.

The Box-spline $M_{\mathcal{D}_n}$. The $n(n-1)$-directions of the box-spline on the $\mathcal{D}_n$ lattice are the non-parallel directions of $\mathscr{D}_n$:

$$\boldsymbol{\Xi}_{\mathcal{D}_n} := \bigcup_{1 \leq i < j \leq n} \left\{ \mathbf{e}_n^i \pm \mathbf{e}_n^j \right\}.$$

The centered and re-normalized box-spline is defined as

$$M_{\mathcal{D}_n} := |\det \mathbf{G}_{\mathcal{D}_n}| M^c_{\boldsymbol{\Xi}_{\mathcal{D}_n}} = |\det \mathbf{G}_{\mathcal{D}_n}| M_{\boldsymbol{\Xi}_{\mathcal{D}_n}}(\cdot + \sum_{\boldsymbol{\xi} \in \boldsymbol{\Xi}_{\mathcal{D}_n}} \boldsymbol{\xi}/2).$$

The following lemma will be helpful to prove the properties of $M_{\mathcal{D}_n}$.

Lemma 4. *Let* $\boldsymbol{\Xi}^{\perp \boldsymbol{v}} := \{\boldsymbol{\xi} \in \boldsymbol{\Xi} : \boldsymbol{\xi} \cdot \boldsymbol{v} = 0\}$. *Then*

$$\max_{\boldsymbol{v}\in\mathbb{R}^n} \#\boldsymbol{\Xi}_{\mathcal{D}_n}^{\perp \boldsymbol{v}} = \begin{cases} 3 & (n=3) \\ (n-1)(n-2) & (n>3). \end{cases}$$

Proof. As in the proof of Lemma 3, we find an upper bound of $\#\boldsymbol{\Xi}_{\mathcal{D}_n}^{\perp \boldsymbol{v}}$ and exhibit a vector $\boldsymbol{v}$ so that the bound is taken on.

For $\boldsymbol{v} \in \mathbb{R}^n$, $\boldsymbol{v} \neq \mathbf{0}_n$, let, without loss of generality since we can rearrange rows in $\boldsymbol{\Xi}_{\mathcal{D}_n}$, the set of nonzero element indices be $\{j \in \mathbb{Z} : \boldsymbol{v} \in \mathbb{R}^n, \boldsymbol{v}(j) \neq 0\} = \{1, \ldots, k\}$, where $0 < k \leq n$.

We decompose $\boldsymbol{\Xi}_{\mathcal{D}_n}$ into three disjoint subsets as

$$\boldsymbol{\Xi}_{\mathcal{D}_n} = \mathbf{Z}_1 \sqcup \mathbf{Z}_2 \sqcup \mathbf{Z}_3, \qquad \text{where} \qquad \begin{aligned} \mathbf{Z}_1 &:= \{\mathbf{e}_n^i \pm \mathbf{e}_n^j : 1 \leq i < j \leq k\} \\ \mathbf{Z}_2 &:= \{\mathbf{e}_n^i \pm \mathbf{e}_n^j : 1 \leq i \leq k < j \leq n\} \\ \mathbf{Z}_3 &:= \{\mathbf{e}_n^i \pm \mathbf{e}_n^j : k < i < j \leq n\}. \end{aligned}$$

Since $\mathbf{Z}_1 = \emptyset$ for $k = 1$ and either $(\mathbf{e}_n^i + \mathbf{e}_n^j) \cdot \boldsymbol{v} \neq 0$ or $(\mathbf{e}_n^i - \mathbf{e}_n^j) \cdot \boldsymbol{v} \neq 0$ for $\{\mathbf{e}_n^i \pm \mathbf{e}_n^j\} \subset \mathbf{Z}_1$ and $k > 1$,

$$\#\mathbf{Z}_1^{\perp \boldsymbol{v}} \begin{cases} = 0 & (k=1) \\ \leq \#\mathbf{Z}_1/2 = \binom{k}{2} & \text{otherwise.} \end{cases}$$

For $\mathbf{e}_n^i \pm \mathbf{e}_n^j \in \mathbf{Z}_2$ since $(\mathbf{e}_n^i \pm \mathbf{e}_n^j) \cdot \boldsymbol{v} = \boldsymbol{v}(i) \neq 0$, $\#\mathbf{Z}_2^{\perp \boldsymbol{v}} = 0$. And

$$\#\mathbf{Z}_3^{\perp \boldsymbol{v}} = \begin{cases} 0 & (k \geq n-1) \\ \#\mathbf{Z}_3 = 2\binom{n-k}{2} & \text{otherwise.} \end{cases}$$

Therefore,

(i) if $k = 1$, $\#\boldsymbol{\Xi}_{\mathcal{D}_n}^{\perp \boldsymbol{v}} = \#(\mathbf{Z}_2 \sqcup \mathbf{Z}_3)^{\perp \boldsymbol{v}} = \#\mathbf{Z}_2^{\perp \boldsymbol{v}} + \#\mathbf{Z}_3^{\perp \boldsymbol{v}} = 2\binom{n-1}{2} = (n-1)(n-2) =: f(n)$;

(ii) if $k \geq n-1$, $\#\boldsymbol{\Xi}_{\mathcal{D}_n}^{\perp \boldsymbol{v}} = \#(\mathbf{Z}_1 \sqcup \mathbf{Z}_2)^{\perp \boldsymbol{v}} = \#\mathbf{Z}_1^{\perp \boldsymbol{v}} + \#\mathbf{Z}_2^{\perp \boldsymbol{v}} \leq \binom{k}{2} = \frac{1}{2}k(k-1)$

$$= \begin{cases} \frac{1}{2}(n-1)(n-2) = f(n)/2 & (k = n-1) \\ \frac{1}{2}n(n-1) =: f(n+1)/2 & (k = n); \end{cases}$$

(iii) if $2 \leq k \leq n-2$, define $j := n-2-k$ and $l := n-j-4$. Since $k \geq 2$ and $n \geq 4$ by assumption, $0 \leq j \leq n-4$ and $l \geq 0$. Substituting $n = j+4+l$ and $k = n-2-j = 2+l$ yields

$$\binom{k}{2} + 2\binom{n-k}{2} - f(n) = -\frac{1}{2}(l^2 + 7l + 4j + 4jl + 6) < 0$$

and hence

$$\#\boldsymbol{\Xi}_{\mathcal{D}_n}^{\perp \boldsymbol{v}} = \#\mathbf{Z}_1^{\perp \boldsymbol{v}} + \#\mathbf{Z}_2^{\perp \boldsymbol{v}} + \#\mathbf{Z}_3^{\perp \boldsymbol{v}} \qquad \leq \binom{k}{2} + 2\binom{n-k}{2} \leq f(n).$$

Since $f(n+1) = f(n)\frac{n}{n-2}$, $\#\boldsymbol{\Xi}_{\mathcal{D}_n}^{\perp \boldsymbol{v}}$ is maximized by $f(3+1)/2 = 3$ for $n = 3$ and $f(n)$ for $n > 3$. The bound is sharp since

$$\max_{\boldsymbol{v}\in\mathbb{R}^n} \#\boldsymbol{\Xi}_{\mathcal{D}_3}^{\perp \boldsymbol{v}} = \#\boldsymbol{\Xi}_{\mathcal{D}_3}^{\perp \mathbf{j}_n} = 3$$

and for $n > 3$,

$$\max_{\boldsymbol{v}\in\mathbb{R}^n} \#\boldsymbol{\Xi}_{\mathcal{D}_n}^{\perp \boldsymbol{v}} = \#\boldsymbol{\Xi}_{\mathcal{D}_n}^{\perp \mathbf{e}_n^j} = (n-1)(n-2) = f(n)$$

where $1 \le j \le n$. ☐

Theorem 4 (Properties of $M_{\mathcal{D}_n}$)**.** *The box-spline $M_{\mathcal{D}_n}$ has (i) polynomial degree $n(n-2)$, (ii) $M_{\mathcal{D}_3} \in C^1$ and for $n > 3$ $M_{\mathcal{D}_n} \in C^{2n-4}$, and (iii) the sequence $(M_{\mathcal{D}_n}(\cdot - \boldsymbol{j}))_{\boldsymbol{j}\in\mathbf{G}_{\mathcal{D}_n}\mathbb{Z}^n}$ is linearly dependent except for $n = 3$.*

Proof. (i) This follows from $\#\boldsymbol{\Xi}_{\mathcal{D}_n} - n = n(n-1) - n = n(n-2)$.

(ii) By Lemma 4, for $n > 3$, $m(\boldsymbol{\Xi}_{\mathcal{D}_n}) = (n(n-1) - (n-1)(n-2)) - 1 = 2n-3$. So

$$m(\boldsymbol{\Xi}_{\mathcal{D}_n}) = \begin{cases} (6-3)-1 = 2 & (n=3) \\ 2n-3 & (n>3) \end{cases}$$

and $M_{\mathcal{D}_n} \in C^1$ if $n = 3$ and $M_{\mathcal{D}_n} \in C^{2n-4}$ if $n > 3$.

(iii) Since (cf. [27])

$$\det \mathbf{G}_{\mathcal{D}_n} = \det \begin{bmatrix} \mathbf{I}_{n-1} & -\mathbf{e}_{n-1}^{n-1} \\ -\mathbf{j}_{n-1}^t & -1 \end{bmatrix} = \det \mathbf{I}_{n-1} \det\left(-1 - \mathbf{j}_{n-1}^t \mathbf{I}_{n-1}^{-1} \mathbf{e}_{n-1}^{n-1}\right) = -2,$$

the sequence is linearly independent if and only if $\det \mathbf{Z} \in \{0, \pm 2\}$, $\quad \forall \mathrm{Z} \subset \boldsymbol{\Xi}_{\mathcal{D}_n}$. But for $\mathbf{Z}_0 \subset \boldsymbol{\Xi}_{\mathcal{D}_n}$,

$$\mathbf{Z}_0 := \begin{cases} \mathbf{Z}_1 & (n \text{ even}) \\ \begin{bmatrix} \mathbf{Z}_1 & & \\ & \begin{smallmatrix} 1 & 1 \\ 1 & -1 \end{smallmatrix} & \begin{smallmatrix} 1 \\ 1 \end{smallmatrix} \end{bmatrix} & (n \text{ odd}) \end{cases} \quad \text{where } \mathbf{Z}_1 := \begin{bmatrix} \mathbf{B} & & \\ & \ddots & \\ & & \mathbf{B} \end{bmatrix} \text{ and } \mathbf{B} := \left[\begin{smallmatrix} 1 & 1 \\ 1 & -1 \end{smallmatrix}\right],$$

$\det \mathbf{Z}_0 = (-2)^{\lfloor n/2 \rfloor}$ by [27]. That is $\det \mathbf{Z}_0 \notin \{0, \pm 2\}$ for $n > 3$.

☐

7.2. Examples

The 6-Direction Box-Spline on the FCC Lattice. In dimension three,

$$\boldsymbol{\Xi}_{\mathcal{D}_3} := \begin{bmatrix} 1 & 1 & 1 & 1 & 0 & 0 \\ 1 & -1 & 0 & 0 & 1 & 1 \\ 0 & 0 & 1 & -1 & 1 & -1 \end{bmatrix} \quad \text{and} \quad \mathbf{G}_{\mathcal{D}_3} := \begin{bmatrix} 1 & 0 & 0 \\ 0 & 1 & 1 \\ -1 & -1 & 1 \end{bmatrix}.$$

Therefore $M_{\mathcal{D}_3} \cong M_{\mathcal{A}_3}^{\pm}$ since it is centered and re-normalized (see Section 5.2).

8. Symmetric $(n+2^{n-1})$-direction Box-Spline on the $\mathcal{D}_n^*$ Lattice

The root lattice $\mathcal{D}_n^*$, the dual of $\mathcal{D}_n$, can be built as a super-lattice of the integer grid (Cartesian lattice) by inserting additional points at the center of each hypercube. It is therefore a second family, besides $\mathcal{A}_n^*$, that includes the BCC lattice. The box-spline $M_{\mathcal{D}_n^*}$ is constructed by the n main axis directions and 2^{n-1} directions to the centers of the 2^n hypercubes around the origin (see Figure 8 for $n=3$). These directions are pairwise parallel to those of the $(n+2^{n-1})$-direction box-spline on the Cartesian lattice, $M_{\mathbb{Z}^n}$, (Section 3) but their lengths are different.

8.1. Lattice, Definition and Properties

The Root lattice $\mathcal{D}_n^*$. Generator matrices for the $\mathcal{D}_n^*$ lattice can be obtained from those for $\mathcal{D}_n$

$$\mathbf{G}_{\mathcal{D}_n}^{-t} = \begin{bmatrix} \mathbf{I}_{n-1} & -\mathbf{e}_{n-1}^{n-1} \\ -\mathbf{j}_{n-1}^t & -1 \end{bmatrix}^{-t} = \begin{bmatrix} \mathbf{I}_{n-2} & \mathbf{0}_{n-2} & \mathbf{0}_{n-2} \\ \mathbf{0}_{n-2}^t & 1 & -1 \\ -\mathbf{j}_{n-2}^t & -1 & -1 \end{bmatrix}^{-t} = \begin{bmatrix} \mathbf{I}_{n-2} & \mathbf{0}_{n-2} & \mathbf{0}_{n-2} \\ -\mathbf{j}_{n-1}^t/2 & 1/2 & -1/2 \\ -\mathbf{j}_{n-1}^t/2 & -1/2 & -1/2 \end{bmatrix}.$$

However, we prefer the simpler equivalent representation for the generator matrix (cf. [10])

$$\mathbf{G}_{\mathcal{D}_n^*} := \frac{1}{2}\mathbf{j}_n \cup \bigcup_{j=1}^{n-1} \mathbf{e}_n^j = \begin{bmatrix} \mathbf{I}_{n-1} & \mathbf{j}_{n-1}/2 \\ \mathbf{0}_{n-1}^t & 1/2 \end{bmatrix}.$$

The Box-spline $M_{\mathcal{D}_n^*}$. The $(n+2^{n-1})$-direction box-spline on the $\mathcal{D}_n^*$ lattice is constructed by the directions implied by the lattice points

$$\mathbf{\Xi}_{\mathcal{D}_n^*} := \mathbf{I}_n \cup \frac{1}{2}\{\mathbf{e}_n^n + \sum_{j=1}^{n-1} \pm \mathbf{e}_n^j\}$$

corresponding to the centers of the 2^n unit cubes adjacent to the origin and the n main axis directions.

The centered and re-normalized box-spline is defined as

$$M_{\mathcal{D}_n^*} := |\det \mathbf{G}_{\mathcal{D}_n^*}| M^c_{\mathbf{\Xi}_{\mathcal{D}_n^*}} = |\det \mathbf{G}_{\mathcal{D}_n^*}| M_{\mathbf{\Xi}_{\mathcal{D}_n^*}}(\cdot + \sum_{\boldsymbol{\xi}\in\mathbf{\Xi}_{\mathcal{D}_n^*}} \boldsymbol{\xi}/2).$$

Theorem 5 (Properties of $M_{\mathcal{D}_n^*}$)**.** *The box-spline $M_{\mathcal{D}_n^*}$ has (i) polynomial degree 2^{n-1}, (ii) $M_{\mathcal{D}_n^*} \in C^{2^{n-2}}$ and (iii) the sequence $\big(M_{\mathcal{D}_n^*}(\cdot - \boldsymbol{j})\big)_{\boldsymbol{j}\in\mathbf{G}_{\mathcal{D}_n^*}\mathbb{Z}^n}$ is linearly dependent.*

Proof. (i) This follows from $\#\mathbf{\Xi}_{\mathcal{D}_n^*} - n = n + 2^{n-1} - n = 2^{n-1}$.

(ii) Since the directions in $\mathbf{\Xi}_{\mathcal{D}_n^*}$ are pairwise parallel to those of $\mathbf{\Xi}_{\mathbb{Z}^n}$ (Section 3), $M_{\mathcal{D}_n^*} \in C^{2^{n-2}}$.

(iii) The claim holds since $\mathbf{I}_n \subset \mathbf{\Xi}_{\mathcal{D}_n^*}$ while $\det \mathbf{G}_{\mathcal{D}_n^*} = 1/2$.

∎

8.2. Examples

The 7-Direction Box-Spline on the BCC Lattice. In dimension three, $\mathcal{D}_3^* \cong \mathcal{A}_3^* \cong$ BCC lattice. With the direction matrix $\mathbf{\Xi}_{\text{bcc}}$ (Figure 8(d)) and the generator matrix $\mathbf{G}_{\text{bcc}}$ (equivalent to $\mathbf{G}_{\mathcal{D}_3^*}$ via unimodular transformation but more symmetric)

$$\mathbf{\Xi}_{\text{bcc}} := \mathbf{\Xi}_{\mathcal{D}_3^*} := \frac{1}{2}\begin{bmatrix} 2 & 0 & 0 & 1 & -1 & 1 & -1 \\ 0 & 2 & 0 & 1 & 1 & -1 & -1 \\ 0 & 0 & 2 & 1 & 1 & 1 & 1 \end{bmatrix}, \quad \mathbf{G}_{\text{bcc}} := \frac{1}{2}\begin{bmatrix} -1 & 1 & 1 \\ 1 & -1 & 1 \\ 1 & 1 & -1 \end{bmatrix},$$

we define

$$M_{\text{bcc}} := M_{\mathcal{D}_3^*} := |\det \mathbf{G}_{\text{bcc}}| M_{\mathbf{\Xi}_{\text{bcc}}}(\cdot + \sum_{\boldsymbol{\xi}\in\mathbf{\Xi}_{\text{bcc}}} \boldsymbol{\xi}/2) = \frac{1}{2} M_{\mathbf{\Xi}_{\text{bcc}}}(\cdot + (\frac{1}{2}, \frac{1}{2}, \frac{3}{2})).$$

Lemma 5. *The quasi-interpolant with optimal approximation order* 4 *for the spline space*

$$S_{\text{bcc}} := \operatorname{span}\left(M_{\text{bcc}}(\cdot - \boldsymbol{j})\right)_{\boldsymbol{j}\in\mathbf{G}_{\text{bcc}}\mathbb{Z}^3}$$

is defined by the functional

$$\lambda_{\text{bcc}} f := (f - \frac{1}{24}\sum_{\boldsymbol{\xi}\in\mathbf{\Xi}_{\text{bcc}}} D_{\boldsymbol{\xi}}^2 f)(\mathbf{0}).$$

Proof. With

$$\widetilde{\mathbf{\Xi}}_{\text{bcc}} := \mathbf{G}_{\text{bcc}}^{-1}\mathbf{\Xi}_{\text{bcc}} = \begin{bmatrix} 0 & 1 & 1 & 1 & 1 & 0 & 0 \\ 1 & 0 & 1 & 1 & 0 & 1 & 0 \\ 1 & 1 & 0 & 1 & 0 & 0 & -1 \end{bmatrix},$$

the quasi-interpolant for the spline space $\operatorname{span}(M^c_{\widetilde{\mathbf{\Xi}}_{\text{bcc}}}(\cdot - \boldsymbol{j}))_{\boldsymbol{j}\in\mathbb{Z}^3}$ is defined by the functional (cf. [18])

$$\begin{aligned}
\widetilde{\lambda}_{\text{bcc}} f :=& (f - \frac{1}{6}(D_1^2 + D_2^2 + D_3^2 + D_1D_2 + D_2D_3 + D_3D_1))(\mathbf{0}) \\
=& (f - \frac{1}{24}((D_1 + D_2 + D_3)^2 + (D_1 + D_2)^2 + (D_2 + D_3)^2 + (D_3 + D_1)^2 \\
& + D_1^2 + D_2^2 + D_3^2) f)(\mathbf{0}) \\
=& (f - \frac{1}{24}\sum_{\boldsymbol{\xi}\in\widetilde{\mathbf{\Xi}}_{\text{bcc}}} D_{\boldsymbol{\xi}}^2 f)(\mathbf{0}).
\end{aligned}$$

By Lemma 2, the quasi-interpolant for the spline space S_{bcc} is defined by $\lambda_{\text{bcc}} f$. $\square$

For a discrete input $f : \mathbf{G}_{\text{bcc}}\mathbb{Z}^3 \to \mathbb{R}$, the discrete quasi-interpolant, using the 7 directions, has the form

$$\lambda_{\text{bcc}}\left(f(\cdot + \boldsymbol{j})\right) \approx \frac{19}{12} f(\boldsymbol{j}) - \frac{1}{24}\sum_{\boldsymbol{\xi}\in\mathbf{\Xi}_{\text{bcc}}} \left(f(\boldsymbol{j}+\boldsymbol{\xi}) + f(\boldsymbol{j}-\boldsymbol{\xi})\right).$$

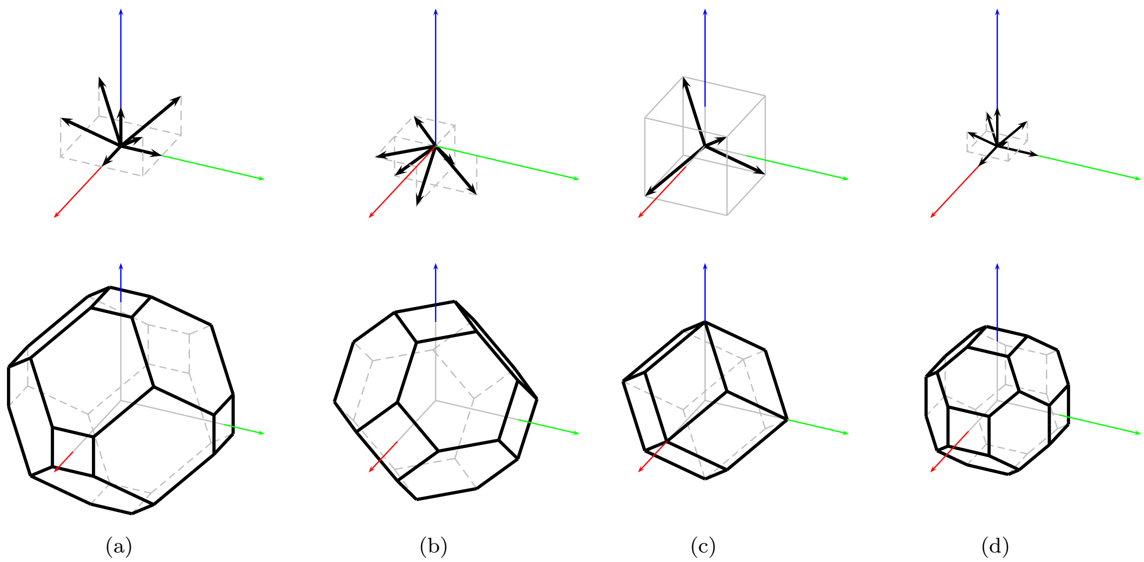

Figure 8. Trivariate symmetric box-splines (top) directions (bottom) supports. (a) 7-direction box-spline on $\mathbb{Z}^3$ (Section 3.2) (b) 6-direction box-spline on the FCC lattice (Section 5.2 and Section 7.2), (c) 4-direction box-spline on the BCC lattice (Section 6) and (d) 7-direction box-spline on the BCC lattice (Section 8.2).

9. Summary and Conclusion

We derived families of symmetric box-spline reconstruction filters for the irreducible root lattices that exist in any number of dimensions by convolution in directions intrinsic to each lattice. This generalizes the known constructions in two and three variables. Table 3 summarizes the findings of this paper, the polynomial degree, continuity, linear independence and optimal quasi-interpolants. For computation, we also point to Kim and Peters [20] where explicit BB-coefficients are derived for specific low-dimensional box-splines and an algorithm for deriving the BB-coefficients in the general case.

Acknowledgment

D. Groisser and A. Entezari gave feedback on an early version of the manuscript. This work was supported in part by NSF Grant CCF-0728797.

[1] D. P. Petersen, D. Middleton, Sampling and Reconstruction of Wave-Number-Limited Functions in N-Dimensional Euclidean Spaces, Information and Control 5 (4) (1962) 279–323.

[2] T. Meng, B. Smith, A. Entezari, A. E. Kirkpatrick, D. Weiskopf, L. Kalantari, T. Möller, On visual quality of optimal 3D sampling and reconstruction, in: GI '07: Proceedings of Graphics Interface 2007, ACM, New York, NY, USA, 265–272, 2007.

Table 3. Symmetric Box-splines on the root lattices. (Cartesian lattice non-Cartesian lattice)

dim.	lattice	box-spline	related to	direction matrix	polynomial degree	approximation order	basis?	quasi-interpolant functional
n	Cartesian	$M_{\mathbb{Z}^n}$		$\mathbf{I}_n \cup \{\mathbf{e}_n^n + \sum_{j=1}^{n-1} \sigma_j \mathbf{e}_n^j : \sigma_j \in \{\pm 1\}\}$	2^{n-1}	$2^{n-2}+2$	no	
2		$M_{\mathbb{Z}^2}$	ZP-element [14]	$\begin{bmatrix} 1 & 0 & 1 & -1 \\ 0 & 1 & 1 & 1 \end{bmatrix}$	2	3	no	$(f - \frac{1}{24}\sum_{\boldsymbol{\xi}\in\boldsymbol{\Xi}_{\mathrm{ZP}}} D_{\boldsymbol{\xi}}^2 f)(\boldsymbol{j})$
3		$M_{\mathbb{Z}^3}$	7-dir. box-spline[4]	$\begin{bmatrix} 1 & 0 & 0 & 1 & -1 & 1 & -1 \\ 0 & 1 & 0 & 1 & 1 & -1 & -1 \\ 0 & 0 & 1 & 1 & 1 & 1 & 1 \end{bmatrix}$	4	4	no	$(f - \frac{1}{24}\sum_{\boldsymbol{\xi}\in\boldsymbol{\Xi}_{\mathbb{Z}^3}} D_{\boldsymbol{\xi}}^2 f)(\boldsymbol{j})$
n	$\mathcal{A}_n$	$M_{\mathcal{A}_n}^{\pm}$		$\bigcup_{1\le i<j\le n+1} \left\{\mathbf{X}_n^{\pm}(\mathbf{e}_{n+1}^i - \mathbf{e}_{n+1}^j)\right\}$	$\frac{n(n-1)}{2}$	n	yes	
2	hexagonal	$M_{\mathcal{A}_2}^{\pm}$	hat functions	$\frac{1}{2}\begin{bmatrix} 2 & 1\pm\sqrt{3} & -1\pm\sqrt{3} \\ -2 & -1\pm\sqrt{3} & 1\pm\sqrt{3} \end{bmatrix}$	1	2	yes	$f(\boldsymbol{j})$
3	FCC	$M_{\mathcal{A}_3}^{-}$	6-dir. box-spline[8]	$\begin{bmatrix} 1 & 1 & 0 & 0 & -1 & -1 \\ -1 & 0 & -1 & 1 & 0 & -1 \\ 0 & -1 & -1 & -1 & -1 & 0 \end{bmatrix}$	3	3	yes	$(f - \frac{1}{24}\sum_{\boldsymbol{\xi}\in\boldsymbol{\Xi}_{\mathrm{fcc}}} D_{\boldsymbol{\xi}}^2 f)(\boldsymbol{j})$
n	$\mathcal{A}_n^*$	$M_{\mathcal{A}_n^*}^{\pm}$		$\mathbf{A}_n^{*\pm}\begin{bmatrix} \mathbf{I}_n & -\mathbf{j}_n \end{bmatrix}$	1	2	yes	$f(\boldsymbol{j})$
n	$\mathcal{A}_n^*$	$M_r^{*\pm}$		$\mathbf{A}_n^{*\pm}\bigcup_{i=1}^{r}\begin{bmatrix} \mathbf{I}_n & -\mathbf{j}_n \end{bmatrix}$	$r(n+1)-n$	$2r$	yes	
n	$\mathcal{A}_n^*$	$M_2^{*\pm}$		$\mathbf{A}_n^{*\pm}\begin{bmatrix} \mathbf{I}_n & -\mathbf{j}_n & \mathbf{I}_n & -\mathbf{j}_n \end{bmatrix}$	$n+2$	4	yes	$(f - \frac{1}{12}\sum_{\boldsymbol{\xi}\in\mathbf{T}_2^{*\pm}} D_{\boldsymbol{\xi}}^2 f)(\boldsymbol{j})$
2	hexagonal	$M_{\mathcal{A}_2^*}^{\pm}$		$\frac{1}{2\sqrt{3}}\begin{bmatrix} 1\pm\sqrt{3} & 1\mp\sqrt{3} & 2 \\ 1\mp\sqrt{3} & 1\pm\sqrt{3} & 2 \end{bmatrix}$	1	2	yes	$f(\boldsymbol{j})$
3	BCC	$M_{\mathcal{A}_3^*}^{\pm}$	4-dir. box-spline[6]	$\frac{1}{2}\begin{bmatrix} -1 & 1 & 1 & -1 \\ 1 & -1 & 1 & -1 \\ 1 & 1 & -1 & -1 \end{bmatrix}$	1	2	yes	$f(\boldsymbol{j})$
$n>3$	$\mathcal{D}_n$	$M_{\mathcal{D}_n}$		$\bigcup_{1\le i<j\le n} \{\mathbf{e}_n^i + \mathbf{e}_n^j, \mathbf{e}_n^i - \mathbf{e}_n^j\}$	$n(n-2)$	$2n-2$	no	
3	FCC	$M_{\mathcal{D}_3}$	6-dir. box-spline[8]	$\begin{bmatrix} 1 & 1 & 1 & 1 & 0 & 0 \\ 1 & -1 & 0 & 0 & 1 & 1 \\ 0 & 0 & 1 & -1 & 1 & -1 \end{bmatrix}$	3	3	yes	$(f - \frac{1}{24}\sum_{\boldsymbol{\xi}\in\boldsymbol{\Xi}_{\mathrm{fcc}}} D_{\boldsymbol{\xi}}^2 f)(\boldsymbol{j})$
n	$\mathcal{D}_n^*$	$M_{\mathcal{D}_n^*}$		$\mathbf{I}_n \cup \frac{1}{2}\{\mathbf{e}_n^n + \sum_{j=1}^{n-1} \sigma_j \mathbf{e}_n^j : \sigma_j \in \{\pm 1\}\}$	2^{n-1}	$2^{n-2}+2$	no	
3	BCC	$M_{\mathcal{D}_3^*}$		$\frac{1}{2}\begin{bmatrix} 2 & 0 & 0 & 1 & -1 & 1 & -1 \\ 0 & 2 & 0 & 1 & 1 & -1 & -1 \\ 0 & 0 & 2 & 1 & 1 & 1 & 1 \end{bmatrix}$	4	4	no	$(f - \frac{1}{24}\sum_{\boldsymbol{\xi}\in\boldsymbol{\Xi}_{\mathrm{bcc}}} D_{\boldsymbol{\xi}}^2 f)(\boldsymbol{j})$

[3] D. Van De Ville, T. Blu, M. Unser, W. Philips, I. Lemahieu, R. Van de Walle, Hex-Splines: A Novel Spline Family for Hexagonal Lattices, IEEE Tr. on Image Proc. 13 (6) (2004) 758–772.

[4] J. Peters, C^2 Surfaces Built from Zero Sets of the 7-Direction Box Spline, in: Proc. of the 6th IMA Conf. on the Math. of Surfaces, Clarendon Press, New York, NY, USA, 463–474, 1996.

[5] A. Entezari, T. Möller, Extensions of the Zwart-Powell Box Spline for Volumetric Data Reconstruction on the Cartesian Lattice, IEEE TVCG 12 (5) (2006) 1337–1344.

[6] A. Entezari, R. Dyer, T. Möller, Linear and Cubic Box Splines for the Body Centered Cubic Lattice, in: VIS '04, IEEE Computer Society, 11–18, 2004.

[7] A. Entezari, Optimal Sampling Lattices and Trivariate Box Splines, Ph.D. thesis, Simon Fraser University, 2007.

[8] M. Kim, A. Entezari, J. Peters, Box Spline Reconstruction on the Face-Centered Cubic Lattice, IEEE Transactions on Visualization and Computer Graphics (Proceedings Visualization / Information Visualization 2008) 14 (6) (2008) 1523–1530.

[9] M. Kim, Symmetric Box-Splines on Root Lattices, Ph.D. thesis, University of Florida, 2008.

[10] J. H. Conway, N. J. A. Sloane, Sphere Packings, Lattices and Groups, Springer-Verlag New York, Inc., New York, NY, USA, 3rd edn., 1998.

[11] C. de Boor, K. Höllig, S. Riemenschneider, Box splines, Springer-Verlag New York, Inc., 1993.

[12] J. Martinet, Perfect Lattices in Euclidean Spaces, Springer-Verlag Berlin Hidelberg, 2003.

[13] P. S. Tom Lyche, Carla Manni, Quasi-interpolation projectors for box splines, Journal of Computational and Applied Mathematics In Press, Corrected Proof, , Available online 22 October 2007.

[14] P. B. Zwart, Multivariate Splines with Nondegenerate Partitions, SIAM Journal on Numerical Analysis 10 (4) (1973) 665–673.

[15] E. Miller, V. Reiner, B. Sturmfels, Geometric combinatorics, vol. 13 of *IAS Park City Mathematics Series*, AMS Bookstore, ISBN 0821837362, 2007.

[16] C. de Boor, B–form basics, in: G. E. Farin (Ed.), Geometric modeling: Algorithms and New Trends, SIAM, Philadelphia, PA, 131–148, 1987.

[17] C. K. Chui, M.-J. Lai, Algorithms for Generating B-nets and Graphically Displaying Spline Surfaces on Three- and Four-directional Meshes, CAGD 8 (6) (1991) 479–493.

[18] M. Kim, J. Peters, Derivation of Some Quasi-interpolants for Symmetric Box Splines on Root Lattices, Tech. Rep. REP-2010-506, Dept. of CISE, University of Florida, USA, 2010.

[19] J. Peters, M. Wittman, Box-spline based CSG blends, in: Proceedings of the fourth ACM symposium on Solid modeling and applications, SIGGRAPH, ACM Press, 195–205, 1997.

[20] M. Kim, J. Peters, Fast and stable evaluation of box-splines via the Bernstein-Bézier form, Numerical Algorithms 50 (4) (2009) 381–399.

[21] C. de Boor, K. Höllig, Approximation Order from Bivariate C^1-Cubics: A Counterexample, Proceedings of the American Mathematical Society 87 (4) (1983) 649–655.

[22] R. Kane, Reflection Groups and Invariant Theory, Springer-Verlag New York, Inc., 2001.

[23] M. Kim, J. Peters, Symmetric Box-splines on the $\mathcal{A}_n^*$ Lattice, J of Approx Theory 162 (9) (2010) 1607–1630.

[24] R. M. Mersereau, The processing of hexagonally sampled two-dimensional signals, Proceedings of IEEE 67 (6) (1979) 930–949.

[25] H. R. Künsch, E. Agrell, F. A. Hamprecht, Optimal lattices for sampling, IEEE Transactions on Information Theory 51 (2) (2005) 634–647.

[26] H. S. M. Coxeter, Regular polytopes, Dover Publications Inc., New York, third edn., 1973.

[27] J. R. Silvester, Determinants of Block Matrices, Math. Gazette 84 (501) (2000) 460–467.